DPhG ARCH PHARM
Archiv der Pharmazie

Design, synthesis, molecular docking, anticancer evaluations, and in silico pharmacokinetic studies of novel 5-[(4-chloro/2,4-dichloro)benzylidene]thiazolidine-2,4-dione derivatives as VEGFR-2 inhibitors

Khaled El-Adl[1,2] ⓘ | Abdel-Ghany A. El-Helby[1] | Helmy Sakr[1] | Rezk R. Ayyad[1] | Hazem A. Mahdy[1] | Mohamed Nasser[1] | Hamada S. Abulkhair[3,4] ⓘ | Sanadelaslam S. A. El-Hddad[1]

[1]Pharmaceutical Medicinal Chemistry and Drug Design Department, Faculty of Pharmacy (Boys), Al-Azhar University, Cairo, Egypt

[2]Pharmaceutical Chemistry Department, Faculty of Pharmacy, Heliopolis University for Sustainable Development, Cairo, Egypt

[3]Pharmaceutical Organic Chemistry Department, Faculty of Pharmacy (Boys), Al-Azhar University, Cairo, Egypt

[4]Pharmaceutical Chemistry Department, Faculty of Pharmacy, Horus University, New Damietta, Egypt

Correspondence
Khaled El-Adl, Pharmaceutical Medicinal Chemistry and Drug Design Department, Faculty of Pharmacy (Boys), Al-Azhar University, Nasr City 11884, Cairo, Egypt.
Email: eladlkhaled74@yahoo.com, eladlkhaled74@azhar.edu.eg and khaled.eladl@hu.edu.eg

Abstract

The anticancer activity of novel thiazolidine-2,4-diones was evaluated against HepG2, HCT-116, and MCF-7 cells. MCF-7 was the most sensitive cell line to the cytotoxicity of the new derivatives. In particular, compounds **18**, **12**, **17**, and **16** were found to be the most potent derivatives over all the tested compounds against the cancer cell lines HepG2, HCT116, and MCF-7, with IC_{50} = 9.16 ± 0.9, 8.98 ± 0.7, 5.49 ± 0.5 µM; 9.19 ± 0.5, 8.40 ± 0.7, 6.10 ± 0.4 µM; 10.78 ± 1.2, 8.87 ± 1.5, 7.08 ± 1.6 µM; and 10.87 ± 0.8, 9.05 ± 0.7, 7.32 ± 0.4 µM, respectively. Compounds **18** and **12** have nearly the same activities as sorafenib (IC_{50} = 9.18 ± 0.6, 5.47 ± 0.3, and 7.26 ± 0.3 µM, respectively), against HepG2 cells, but slightly lower activity against HCT116 cells and slightly higher activity against the MCF-7 cancer cell line. Also, these compounds displayed lower activities than doxorubicin against HepG2 and HCT-116 cells but higher activity against MCF-7 cells (IC_{50} = 7.94 ± 0.6, 8.07 ± 0.8, and 6.75 ± 0.4 µM, respectively). In contrast, compounds **17** and **16** exhibited lower activities than sorafenib against HepG2 and HCT116 cells, but nearly equipotent activity against the MCF-7 cancer cell line. Also, these compounds displayed lower activities than doxorubicin against the three cell lines. All the synthesized derivatives **7–18** were evaluated for their inhibitory activities against VEGFR-2. The tested compounds displayed high to medium inhibitory activity, with IC_{50} values ranging from 0.17 ± 0.02 to 0.27 ± 0.03 µM. Compounds **18**, **12**, **17**, and **16** potently inhibited VEGFR-2 at IC_{50} values of 0.17 ± 0.02, 0.17 ± 0.02, 0.18 ± 0.02, and 0.18 ± 0.02 µM, respectively, which are nearly more than half of that of the IC_{50} value for sorafenib (0.10 ± 0.02 µM).

KEYWORDS
anticancer agents, molecular docking, thiazolidine-2-4-dione, VEGFR-2 inhibitors

1 | INTRODUCTION

The developments in cancer therapies have focused on molecular targets, particularly tumor angiogenesis.[1] Angiogenesis is the process by which the existing vascular bed expands to form new blood vessels and is a pivotal event in many physiological and pathological processes, including tumor growth and metastasis.[2,3] Newly generated blood vessels supply oxygen and essential nutrition, support tumor growth, and later aid in the initiation of metastasis, which contributes to more than 90% of deaths in various cancers.[4] The thiazolidine-2,4-diones (TZDs) have exhibited antitumor activity in a wide variety of experimental cancer models by affecting cell cycle, induction of cell differentiation, and apoptosis as well as by inhibiting tumor angiogenesis. TZD scaffold has been proposed for hybridization with different bioactive moieties to have a different mechanism of action with a broad spectrum of activity against numerous cancer cell lines.[5,6] Vascular endothelial growth factor (VEGF) is one of the central regulators in angiogenesis.[7] Vascular endothelial growth factor receptor-2 (VEGFR-2) is the receptor for VEGF and is the prime mediator of VEGF-induced pro-angiogenesis signaling.[8] Binding of VEGF to VEGFR-2 leads to the dimerization of the receptors, activation of tyrosine kinase, trans-autophosphorylation, and initiation of the extracellular signal-regulated kinase.[9–11] Considering that angiogenesis is a significant event in tumor development, blocking angiogenesis is one of the most promising strategies to treat malignancies. A study reported by Shah et al.,[12] showed that TZD derivative ciglitazone (I) (Figure 1) significantly decreased the VEGF production in human granulose cells in an in vitro model. Extensive studies were reported in the synthesis of several 5-benzylidenethiazolidine-2,4-dione derivatives as potent anticancer agents[13–20] and potent VEGFR-2 inhibitors, for example, compound II.[2,12] Owing to the importance of VEGFR-2 in angiogenesis, this receptor is the most vital target in anti-angiogenic therapy against cancer. Numerous reports on VEGFR-2 inhibitors, including the commercialized sunitinib (III) (Figure 1), have been published.[21,22] Sorafenib (Nexavar®; IV; (Figure 1) also is a potent VEGFR-2 inhibitor and has been approved as an anti-angiogenic drug.[23–25] Our reported compounds V[19] and VI[20] encourage us to synthesize new derivatives with the hydrophobic electron-withdrawing mono-, chloro-, and/or dichlorobenzylidene instead of unsubstituted (V) or the hydrophobic electron-donating methoxybenzylidenes (VI), respectively, to study the effect of these modifications on the activity.

Study of the structure–activity relationships (SARs) and common pharmacophoric features shared by sorafenib and various VEGFR-2 inhibitors revealed that most VEGFR-2 inhibitors shared four main features as shown in Figure 2[26–28]: (a) the flat heteroaromatic ring system that contains at least one N atom, (b) a central aryl ring (hydrophobic spacer).[29] (c) A linker containing a functional group acting as pharmacophore (e.g., amino or urea) that possesses both H-bond acceptor (HBA) and donor (HBD) to bind with two crucial residues (Glu883 and Asp1044). The NH motifs of the urea or amide moiety usually form one hydrogen bond with Glu883, whereas the C=O motif forms another hydrogen bond with Asp1044. (iv) The terminal hydrophobic moiety of the inhibitors occupies the newly created allosteric hydrophobic pocket. Thus, hydrophobic interactions are usually attained in this allosteric binding region.[30] Furthermore, analysis of the X-ray structure of various inhibitors bound to VEGFR-2 confirmed the sufficient space available for various substituents around the terminal heteroaromatic ring.[31–33]

Ciglitazone (I)

Compound (II)

Sunitinib (III)

Sorafenib (IV)

Compound (V)

Compound (VI)
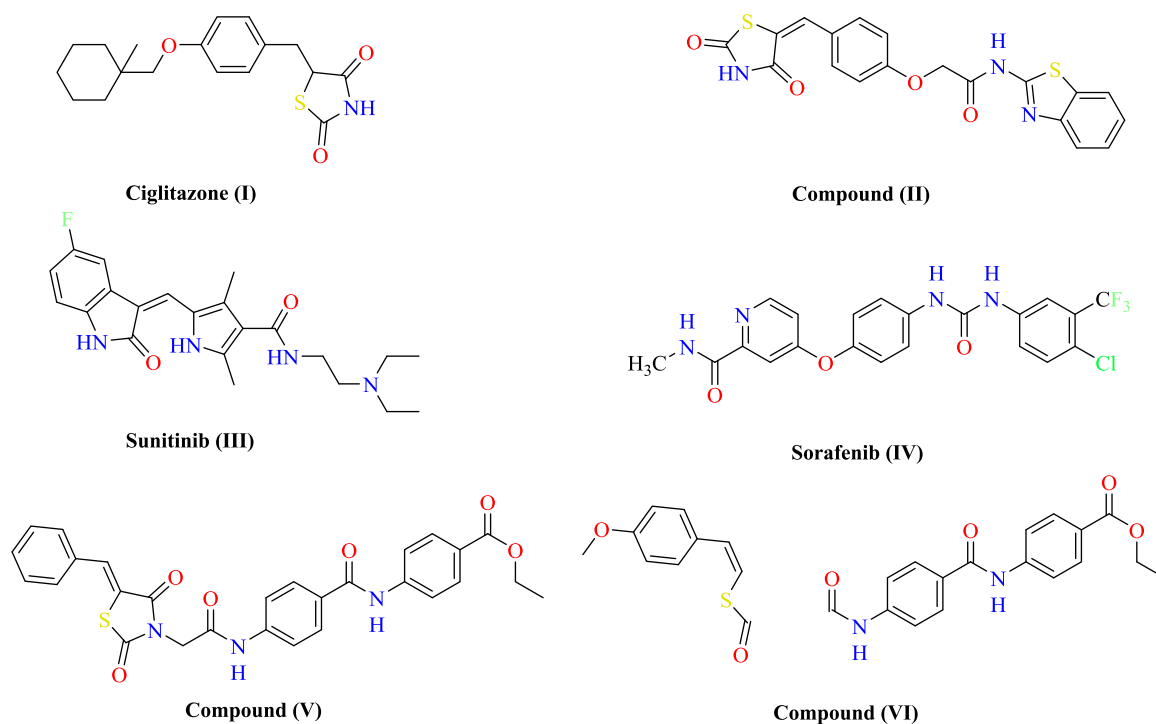
FIGURE 1 Reported vascular endothelial growth factor receptor-2 inhibitors
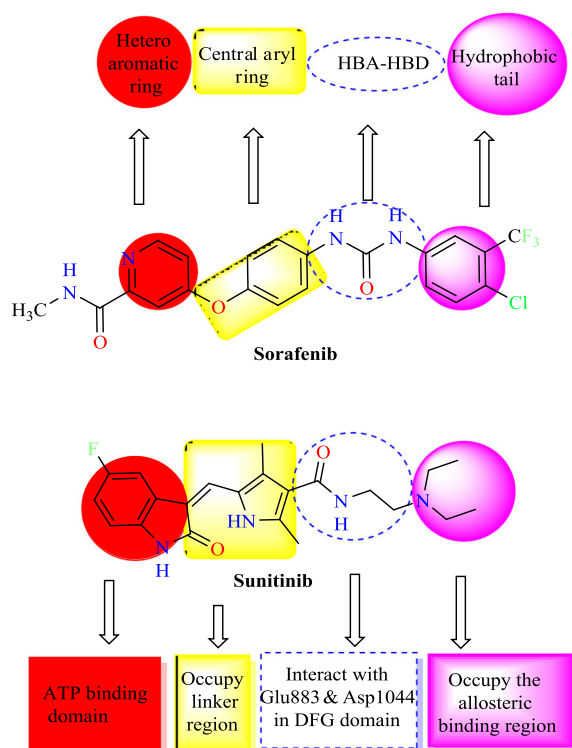
FIGURE 2 The basic structural requirements for sorafenib and sunitinib as reported VEGFR-2 inhibitors. ATP, adenosine triphosphate; HBA, H-bond acceptor; HBD, H-bond donor; VEGFR-2, vascular endothelial growth factor receptor-2

Depending on ligand-based drug design, particularly a molecular hybridization approach that involves the coupling of two or more groups with relevant biological properties,[34] molecular hybridization of 5-([4-chloro/2,4-dichloro]benzylidene)thiazolidine-2,4-diones and other effective antitumor moieties were carried out in an attempt to get new molecules with promising antitumor activities.

In continuation of our efforts to obtain new anticancer agents targeting VEGFR-2, the goal of our work was the synthesis of new agents with the same essential pharmacophoric features of the reported and clinically used VEGFR-2 inhibitors (e.g., sorafenib). The main core of our molecular design rationale comprised bioisosteric modification strategies of VEGFR-2 inhibitors at four different positions (Figure 3).

Our target compounds were designed to have TZD spacers and amide linkers having HBA-HBD, the main pharmacophoric feature in sorafenib hoping to obtain more potent VEGFR-2 inhibitors. First, the bioisosteric approach was adopted in the target 4-chloro and/or 2,4-dichlorobenzylidene to replace the pyridine ring. The second strategy is to use TZD to replace the central aryl ring of lead structure aiming to increase VEGFR-2 binding affinity. The third strategy is using acetamide linkers containing HBA-HBD functional groups that possess HBAs and/or HBDs. Also, the hydrophobic substituted phenyl tail of the reported ligand sorafenib was substituted by other distal hydrophobic moieties that occupied the newly formed hydrophobic groove (Figure 4). Furthermore, the substitution pattern was selected

to ensure different electronic and lipophilic environments, which could influence the activity of the target compounds. These modifications were performed to carry out further elaboration of the TZD scaffolds and to explore a valuable SAR. The designed target 5-([4-chloro/2,4-dichloro]benzylidene)thiazolidine-2,4-dione derivatives were synthesized and evaluated as potential VEGFR-2 inhibitory and antitumor activities against three human tumor cell lines, namely, hepatocellular carcinoma (HCC) type (HepG2), breast cancer (Michigan Cancer Foundation-7 [MCF-7]), and human colorectal carcinoma-116 (HCT-116).

2 | RESULTS AND DISCUSSION

2.1 | Rationale and structure-based design

5-([4-Chloro/2,4-dichloro]benzylidene)thiazolidine-2,4-dione derivatives have the essential pharmacophoric features of VEGFR-2 inhibitors[35–39] (Figure 3), which include the presence of five-membered hetero ring, TZD, substituted with 4-chlorobenzylidene and/or 2,4-dichlorobenzylidene moieties, as hydrophobic portions, forming 5-(4-chlorobenzylidene)thiazolidine-2,4-dione and 5-(2,4-dichlorobenzylidene)thiazolidine-2,4-dione scaffolds linked to substituted hydrophobic phenyl tail through acetamide linkers containing HBA-HBD, which interacts as HBA through its C=O and as H-bond donor through its NH with the essential amino acid residues Asp1044 and Glu883, respectively. Also, the substituted hydrophobic phenyl tails formed hydrophobic bonding interactions with the hydrophobic pocket formed by Asp1044, Cys1043, Ile1042, Hie1024, Leu1017, Val897, Leu887, Lys866, and Glu883. The hydrophobic phenyl tail was substituted with distal hydrophobic moieties through amide linkers to increase the length of the structure to enable the distal phenyl moieties to occupy new hydrophobic grooves formed by Arg1025, Ile1023, Cys1022, Leu1017, Ile890, and Ile886. In addition, 4-chlorobenzylidene and/or 2,4-dichlorobenzylidene moieties were designed to replace the pyridine and 5-fluoro-2-oxoindolin-3-ylidene moieties of the reference ligands sorafenib and sunitinib, respectively. Moreover, TZD was designed to replace the central aryl and the five-membered pyrrole rings of the reference ligands sorafenib and sunitinib, respectively. Furthermore, the hydrophobic 4-chlorobenzylidene and/or 2,4-dichlorobenzylidene moieties occupied the hydrophobic groove formed by Leu1033, Gly920, Lys918, Cys917, Phe916, Glu915, Ala864, and Leu838. In contrast, the TZD moiety occupied the hydrophobic pocket formed by Cys1043, Leu1033, Val914, Val897, and Lys866 (Figures 4 and 5).

2.2 | Chemistry

The synthetic strategy for the preparation of the target compounds (7–18) is depicted in Scheme 1. The synthesis was initiated by the cyclocondensation of thiourea with chloroacetic
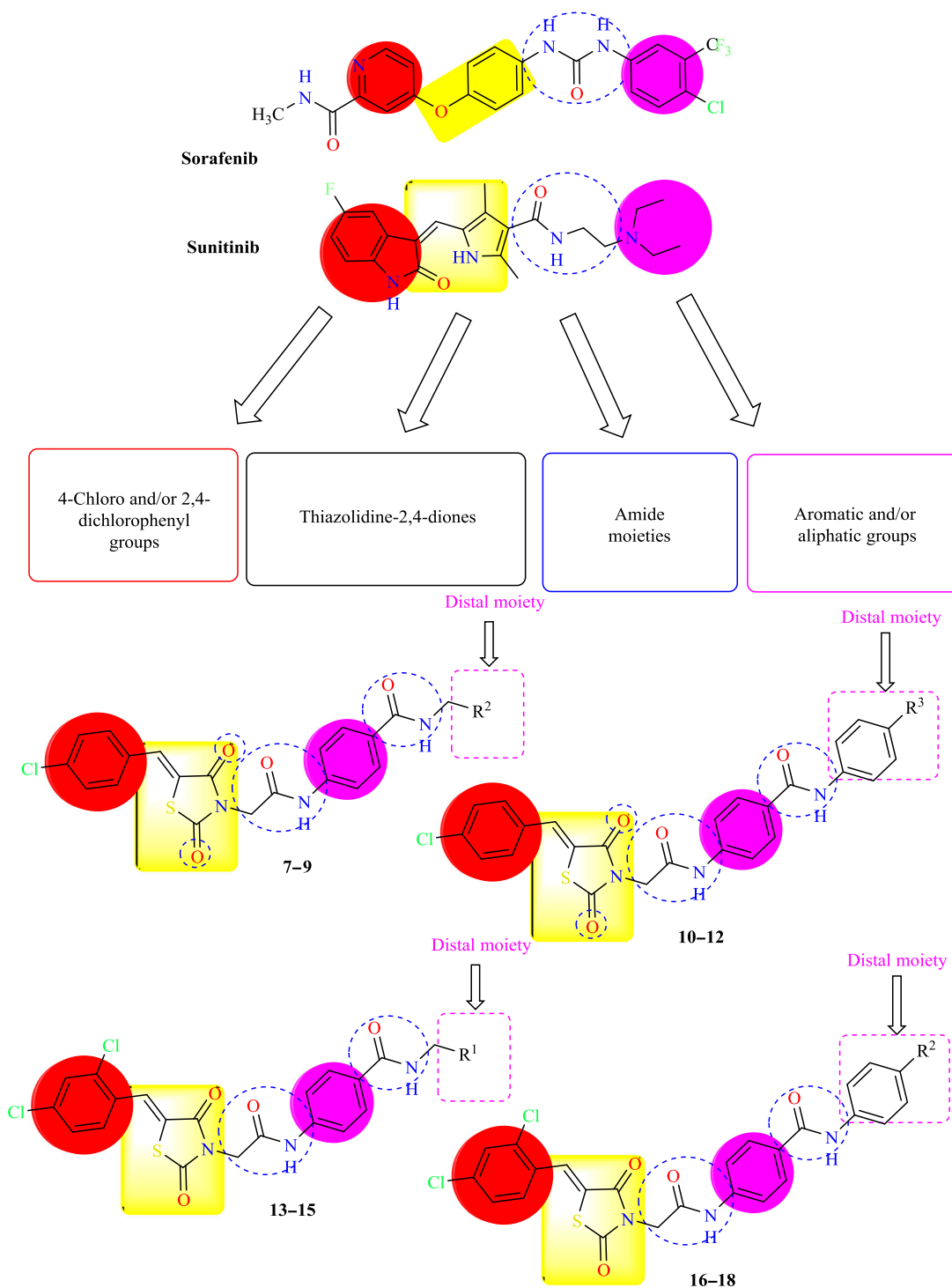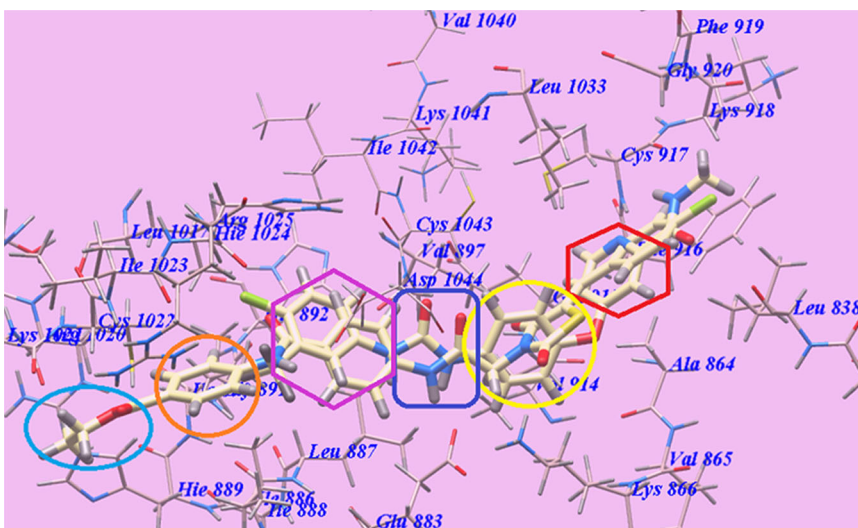
FIGURE 3 Structural similarities and pharmacophoric features of vascular endothelial growth factor receptor-2 inhibitors and designed compounds

acid to afford TZD (**1**),[40,41] which underwent further condensation reaction with the appropriate benzaldehyde, namely, 4-chlorobenzaldehyde and/or 2,4-dichlorobenzaldehyde, to afford the corresponding 5-(4-chlorobenzylidene)thiazolidine-2,4-dione and 5-(2,4-dichlorobenzylidene)thiazolidine-2,4-dione (**2a,b**), respectively, which was heated with alcoholic potassium

hydroxide to afford the corresponding potassium salts (**3a,b**). In contrast, chloroacyl chloride was reacted with 4-aminobenzoic acid (**4**) to obtain the corresponding chloroamide (**5**). The chloroamide **5** was treated with ethyl chloroformate and then the appropriate amine was added to afford the corresponding intermediate (**6a–f**). The potassium salt (**3a,b**) was refluxed with the

FIGURE 4 Superimposition of compound **12** and sorafenib inside the binding pocket of 1YWN
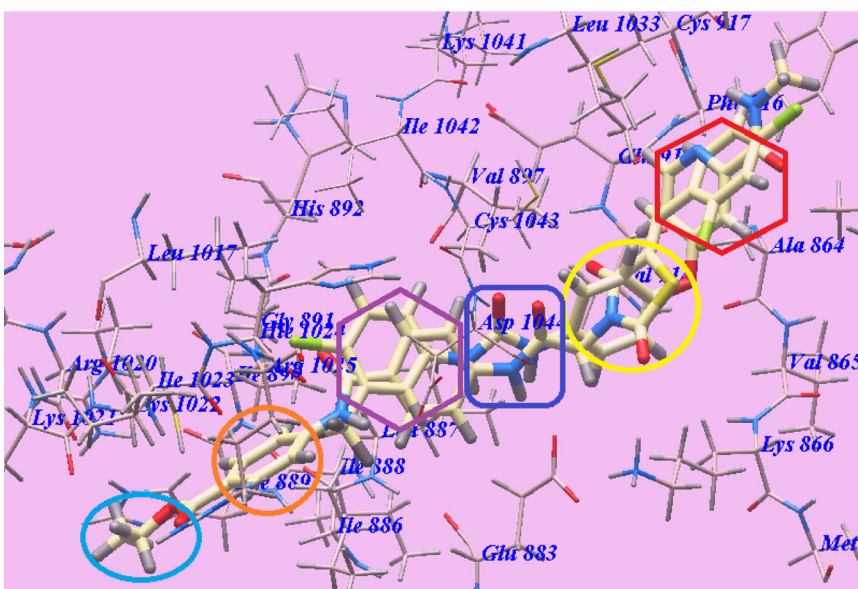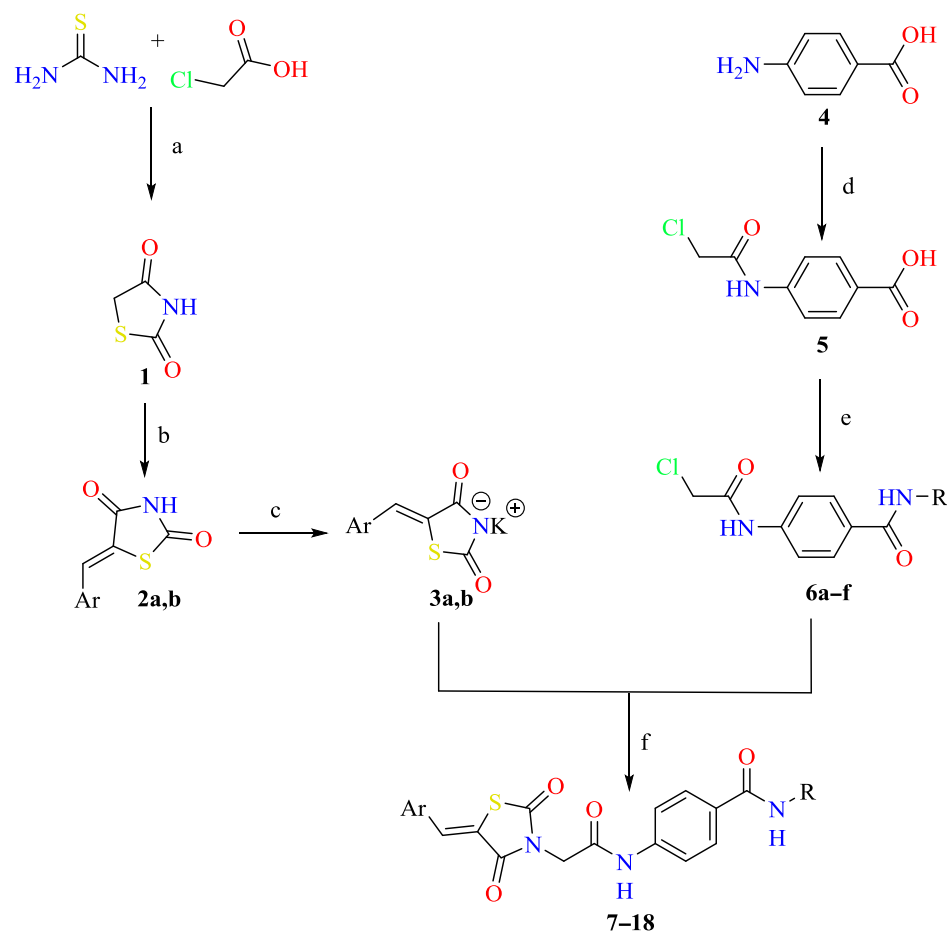

2.3 | Pharmacology/biology

2.3.1 | In vitro cytotoxic activity

Antiproliferative activity of the newly synthesized compounds **7**–**18** was examined against three human tumor cell lines, namely hepatocellular carcinoma (HepG2), colorectal carcinoma (HCT-116), and breast cancer (MCF-7) using the 3-(4,5-dimethylthiazol-2-yl)-2,5-diphenyltetrazolium bromide (MTT) colorimetric assay as described by Mosmann.[42–44] Sorafenib and doxorubicin were included in the experiments as reference cytotoxic drugs. The results were expressed as growth inhibitory concentration (IC_{50}) values, which represented the compound concentrations required to produce a 50% inhibition of cell growth after 72 hr of incubation calculated from the concentration–inhibition response curve and summarized in Table 1. From the obtained results, it was explicated that most of the prepared compounds displayed excellent to modest growth inhibitory activity against the tested cancer cell lines. Investigations of the cytotoxic activity indicated that MCF-7 was the most sensitive cell line to the influence of the new derivatives. In particular, compounds **18**, **12**, **17**, and **16** were found to be the most potent derivatives in all the tested compounds against HepG2, HCT116, and MCF-7 cancer cell lines with IC_{50} = 9.16 ± 0.9, 8.98 ± 0.7, 5.49 ± 0.5 µM; 9.19 ± 0.5, 8.40 ± 0.7, 6.10 ± 0.4 µM; 10.78 ± 1.2, 8.87 ± 1.5, 7.08 ± 1.6 µM; and 10.87 ± 0.8, 9.05 ± 0.7, 7.32 ± 0.4 µM, respectively. Compounds **18** and **12** have nearly the same activities as sorafenib (IC_{50} = 9.18 ± 0.6, 5.47 ± 0.3, and 7.26 ± 0.3 µM, respectively) against the

appropriate intermediate (**6a**–**f**) to obtain the corresponding derivatives **7**–**18**, respectively (Scheme 1).

FIGURE 5 Superimposition of compound **18** and sorafenib inside the binding pocket of 1YWN

Series A, Ar = 4-ClC$_6$H$_4$
7: R = C$_2$H$_5$
8: R = n-C$_3$H$_7$
9: R = n-C$_4$H$_9$
10: R = CH$_2$C$_6$H$_5$
11: R = 4-CH$_3$C$_6$H$_4$
12: R = 4-C$_2$H$_5$OCOC$_6$H$_4$

Series B, Ar = 2,4-Cl$_2$C$_6$H$_3$
13: R = C$_2$H$_5$
14: R = n-C$_3$H$_7$
15: R = n-C$_4$H$_9$
16: R = CH$_2$C$_6$H$_5$
17: R = 4-CH$_3$C$_6$H$_4$
18: R = 4-C$_2$H$_5$OCOC$_6$H$_4$

Reagents and conditions
a) HCl, 90°C, 3hr, 90%;
b) ArCHO/AcOH/AcONa, 90°C, 3hr, 74–80%;
c) KOH/C$_2$H$_5$OH, 90°C, 0.5hr, 95%;
d) ClCH$_2$COCl/DMF/K$_2$CO$_3$, 0–5°C, 1hr, 85%;
e) R^{1}NH$_2$/ECF/TEA/DMF, 0–5°C, 1hr, 80%;
f) TEA/DMF, 90°C, 5hr, 60–85%.

SCHEME 1 Synthetic route for the preparation of the target compounds 7–18

HepG2 cell line, but slightly lower activity against HCT116 and slightly higher activity against MCF-7 cancer cells, respectively. Also, these compounds displayed lower activities than doxorubicin against the HepG2 and HCT-116 cell lines but higher activity against MCF-7 cells, respectively (IC$_{50}$ = 7.94 ± 0.6, 8.07 ± 0.8, and 6.75 ± 0.4 µM, respectively). However, compounds 17 and 16 exhibited lower activities than sorafenib, against HepG2 and HCT116 cells, but nearly equipotent activity against the MCF-7 cancer cell line, respectively. Also, these compounds displayed lower activities than doxorubicin against the three cell lines.

With respect to the HepG2 hepatocellular carcinoma cell line, compounds 8, 9, 10, 11, 14, and 15 displayed very good anticancer activities with IC$_{50}$ ranging from 11.04 ± 1.5 to 19.43 ± 1.8 µM, respectively. Moreover, compounds 7 and 13 with IC$_{50}$ = 21.34 ± 2.1 and 29.37 ± 2.1 µM displayed good cytotoxicity.

Cytotoxicity evaluation against colorectal carcinoma (HCT-116) cell line discovered that compounds 10 and 15 displayed excellent anticancer activities with IC$_{50}$ = 9.35 ± 1.0 and 10.11 ± 0.7 µM, respectively. Compounds 11, 8, 9, and 7 with IC$_{50}$ = 12.71 ± 1.2, 14.89 ± 1.3, 15.03 ± 1.5, and 20.66 ± 1.6 µM displayed very good cytotoxicity. In addition, compound 14 with IC$_{50}$ = 23.66 ± 1.9 µM exhibited good cytotoxicity. While compound 13 with IC$_{50}$ = 34.81 ± 2.4 µM exhibited moderate cytotoxicity.

Cytotoxicity evaluation against the MCF-7 cell line revealed that compounds 10 and 15 displayed excellent anticancer activities with IC$_{50}$ = 7.41 ± 1.4 and 8.21 ± 0.4 µM, respectively. Compounds 11 and 14 with IC$_{50}$ = 12.56 ± 1.2 and 17.72 ± 1.7 µM exhibited very good cytotoxicity. Moreover, compounds 9, 13, and 8 with IC$_{50}$ = 22.08 ± 1.6, 24.11 ± 2.3, and 28.12 ± 1.9 µM exhibited good cytotoxicity.

TABLE 1 In vitro cytotoxic activities of the newly synthesized compounds against the HepG2, HCT-116, and MCF-7 cell lines and VEGFR-2 kinase assay

Compound	IC$_{50}$ (µM)[a]			
	HepG2	HCT116	MCF-7	VEGFR-2
7	21.34 ± 2.1	20.66 ± 1.6	31.12 ± 2.2	0.27 ± 0.03
8	17.13 ± 1.6	14.89 ± 1.3	28.12 ± 1.9	0.23 ± 0.02
9	13.78 ± 1.2	15.03 ± 1.5	22.08 ± 1.6	0.23 ± 0.02
10	11.04 ± 1.5	9.35 ± 1.0	7.41 ± 1.4	0.20 ± 0.02
11	13.52 ± 1.3	12.71 ± 1.2	12.56 ± 1.2	0.19 ± 0.02
12	9.19 ± 0.5	8.40 ± 0.7	6.10 ± 0.4	0.17 ± 0.02
13	29.37 ± 2.1	34.81 ± 2.4	24.11 ± 2.3	0.23 ± 0.02
14	19.43 ± 1.8	23.66 ± 1.9	17.72 ± 1.7	0.22 ± 0.03
15	11.76 ± 0.9	10.11 ± 0.7	8.21 ± 0.4	0.20 ± 0.02
16	10.87 ± 0.8	9.05 ± 0.7	7.32 ± 0.4	0.18 ± 0.02
17	10.78 ± 1.2	8.87 ± 1.5	7.08 ± 1.6	0.18 ± 0.02
18	9.16 ± 0.9	8.98 ± 0.7	5.49 ± 0.5	0.17 ± 0.02
Sorafenib	9.18 ± 0.6	5.47 ± 0.3	7.26 ± 0.3	0.10 ± 0.02
Doxorubicin	7.94 ± 0.6	8.07 ± 0.8	6.75 ± 0.4	NT[b]

[a]IC$_{50}$ values are the mean ± *SD* of three separate experiments.
[b]NT: compounds not tested for their VEGFR-2 inhibitory activity.

While compound **7** with IC$_{50}$ = 31.12 ± 2.2 µM exhibited moderate cytotoxicity.

2.3.2 | In vitro VEGFR-2 kinase assay

All the synthesized derivatives **7**–**18** were evaluated for their inhibitory activities against VEGFR-2 by using an antiphosphotyrosine antibody with the AlphaScreen system (PerkinElmer). The results were reported as a 50% inhibition concentration value (IC$_{50}$) calculated from the concentration–inhibition response curve and summarized in Table 1. Sorafenib was used as a positive control in this assay. The tested compounds displayed high to medium inhibitory activity with IC$_{50}$ values ranging from 0.17 ± 0.02 to 0.27 ± 0.03 µM. Among them, compounds **18**, **12**, **17**, and **16** potently inhibited VEGFR-2 at IC$_{50}$ values of 0.17 ± 0.02, 0.17 ± 0.02, 0.18 ± 0.02, and 0.18 ± 0.02 µM, respectively, which are nearly more than the half of that of sorafenib IC$_{50}$ value (0.10 ± 0.02 µM). Also, compounds **11**, **10**, and **15** possessed very good VEGFR-2 inhibition with IC$_{50}$ values of 0.19 ± 0.02, 0.20 ± 0.02, and 0.20 ± 0.02 µM, respectively, which are nearly half that of sorafenib. Furthermore, compounds **14**, **8**, **9**, **13**, and **7** possessed good VEGFR-2 inhibition with IC$_{50}$ values = 0.22 ± 0.03, 0.23 ± 0.02, 0.23 ± 0.02, 0.23 ± 0.02, and 0.27 ± 0.03 µM, respectively.

2.4 | SAR

The preliminary SAR study has focused on the effect of replacement of the urea and carboxamide linkers of sorafenib and sunitinib, respectively,

with acetamide linkers, which interacts as HBAs through its carbonyl group and as an H-bond donor through its NH atom. These acetamide linkers interact with the side chain NH of the essential amino acid residue Asp1044 and carboxylate of the essential amino acid residue Glu883. Also, hydrophobic interactions through the attached hydrophobic distal moieties were recorded. The effect of replacement of pyridine and 5-fluoro-2-oxoindolin-3-ylidene moieties of sorafenib and sunitinib, respectively, by 4-chlorobenzylidene and/or 2,4-dichlorobenzylidene of 5-([4-chloro/2,4-dichloro]benzylidene)thiazolidine-2,4-dione scaffold of the synthesized compounds on the antitumor activities also was noticed. This 5-([4-chloro/2,4-dichloro]benzylidene moiety occupied the same hydrophobic pocket which was occupied by the pyridine moiety of the standard ligand. Moreover, the TZD was designed to replace the central aryl and pyrrole rings of the reference ligands sorafenib and sunitinib, respectively, and enables the target compounds to form new H-bonds through their 2-carbonyl groups with the essential amino acid residue Lys866. In contrast, different distal aliphatic and aromatic moieties were introduced to the phenyl tail of the reference ligand with different lipophilicity and electronic nature to study their effects on the anticancer activity. The presence of lipophilic distal moieties attached to the phenyl ring through carboxamide linkers formed new hydrophobic and H-bonding interactions with the active site. The data obtained revealed that the tested compounds displayed different levels of anticancer activity and possessed a distinctive pattern of selectivity against the MCF-7 cell lines. Generally, the spacers, linkers (HBA-HBD), lipophilicity, and electronic nature exhibited an important role in anticancer activity. The acetamide and carboxamide linkers were found to be responsible for high anticancer activities. The 2,4-dichlorobenzylidene moiety exhibited higher anticancer activities than the 4-chlorobenzylidene moiety, which may be due to the

higher lipophilicity of the two lipophilic chloro atoms. Compounds with distal phenyl moieties such as **10–12** and **16–18** showed higher activities than those having distal aliphatic ones **7–9** and **13–15** against the three HepG2, HCT116, and MCF-7 cell lines. From the structure of the synthesized derivatives and the data shown in Table 1, we can divide these tested compounds into four groups. The first group has compounds **7–9** that contains 4-chlorobenzylidene moiety. The aliphatic butyl distal moiety **9** showed higher activities than the propyl **8** against both HepG2 and MCF-7 cell lines, respectively, but it showed nearly the same activity against HCT116 cells. Moreover, butyl **9** and propyl **8** derivatives exhibited higher activities than ethyl **7** ones against the three HepG2, HCT116, and MCF-7 cell lines, respectively. The second group has compounds **10–12** with 4-chlorobenzylidene moiety also, the substituted distal phenyl moiety with ethyl ester group as in compound **12** displayed higher activities than that substituted with benzyl moiety **10** and methyl group **11** against the three HepG2, HCT116, and MCF-7 cell lines, respectively. In the third group **13–15** with 2,4-dichlorobenzylidene moiety, the aliphatic butyl distal moiety **15** showed higher activities than the propyl **14** and the ethyl **13** ones against the three HepG2, HCT116, and MCF-7 cell lines, respectively. In the fourth group **16–18** with 2,4-dichlorobenzylidene moiety also, the substituted distal phenyl moiety with ethyl ester group as in compound **18** displayed higher activities than that substituted with methyl group **17** against both HepG2 and MCF-7 cell lines, respectively, but it showed nearly the same activity against HCT116 cell line. Moreover, ethyl ester **18** and toluene derivative **17** derivatives exhibited higher activities than benzyl one **16** against the three HepG2, HCT116, and MCF-7 cell lines, respectively.

The data obtained from the VEGFR-2 inhibition assay concluded that, generally, compounds with 2,4-dichlorobenzylidene moiety exhibited higher VEGFR-2 inhibition activities than those having 4-chlorobenzylidene moiety. The distal phenyl moiety substituted with ethyl ester groups either in 2,4-dichlorobenzylidene or 4-chlorobenzylidene derivatives as in compounds **18** and **12**, respectively, displayed the highest activities at the same IC_{50} value of $0.17 \pm 0.02\,\mu M$. Compounds with distal phenyl moieties such as **10–12** and **16–18** showed higher activities than those having distal aliphatic ones **7–9** and **13–15**, respectively. 2,4-Dichlorobenzylidene with toluene **17** and/or benzylidene **16** distal moieties displayed the same activity at IC_{50} value = $0.18 \pm 0.02\,\mu M$ while toluene derivative **11** in 4-chlorobenzylidene derivatives exhibited higher activity than the benzylidene one **10**. In 2,4-dichlorobenzylidene derivatives, the aliphatic butyl distal moiety **15** displayed higher activity than propyl **14** and ethyl **13** one, respectively. Furthermore, in 4-chlorobenzylidene derivatives the aliphatic butyl distal moiety **9** displayed the same activity as propyl **8**, which was higher than that of ethyl **7** one.

2.5 | Pharmacokinetic profiling study

In the present study, a computational study of the four most active compounds (**12**, **16**, **17**, and **18**) as representative TZDs was conducted to determine the surface area and other physicochemical properties according to the directions of Lipinski's rule.[45] Lipinski suggested that the absorption of a compound is more likely to be better if the molecule achieves at least three out of four of the following rules: (a) HBD groups ≤5, (b) HBA groups ≤10, (c) M.Wt. <500, (d) logP <5. In this study, whereas the reference anticancer agent doxorubicin violates three of Lipinski's rules, compounds **12**, **16**, **17**, and **18** violated only two (M.Wt. and logP). All the highest active derivatives have a number of HBA groups between five and seven and only two HBDs, and these values agree with Lipinski's rules. Also, the absorption, distribution, metabolism, excretion, and toxicity (ADMET) profiles of the newly synthesized TZD derivatives were preliminary assessed to analyze their potentials to build up as good medication candidates. The prediction of ADMET profiles was conducted with the aid of pkCSM descriptors algorithm protocol.[46]

After assessing ADMET profiles of compounds **12**, **16**, **17**, and **18** (Table 2), we can suggest that these derivatives have the advantage of better intestinal absorption in humans than doxorubicin (84.9–95.5, compared with 62.3 in the case of doxorubicin). This preference may be attributed to the superior lipophilicity of our designed ligands, which would make it easier to go along different biological membranes.[47] Accordingly, they may have significantly good bioavailability after oral administration. Studying the central nervous system (CNS) permeability, TZD derivatives **16** and **17** demonstrated the best ability to penetrate the CNS (CNS permeability values approx. −1.7), while doxorubicin is unable to penetrate (CNS permeability < −4.0). It is also clear that cytochrome P3A4, the main enzyme involved in drug metabolism, could be inhibited under the effect of compounds **12**, **16**, **17**, and **18**, while doxorubicin could not. This is also perhaps because of the higher lipophilicity of our new ligands. Excretion was assessed in terms of the total clearance, which is a significant parameter in deciding dose intervals. The obtained data revealed that doxorubicin revealed the highest total clearance value compared with other ligands. In contrast, new ligands showed lower total clearance values (−0.592). Thus, doxorubicin could be excreted quickly and accordingly require shorter dosing intervals. Dissimilar to doxorubicin, new compounds exhibited slower clearance rates, which means the preference of possible extended dosing intervals of the novel thiazolidinediones. The last parameter examined in the ADMET profiles of our newly synthesized VEGFR-2 inhibitors is the toxicity. As displayed in Table 2, doxorubicin and all the new ligands except **18** shared the drawback of unwanted hepatotoxic effects. Gratifyingly, our designed compound **18** showed the great advantage of no expected hepatotoxicity. In terms of the maximum tolerated dose in humans, the new thiazolidinediones **17** and **18** showed more than eightfold of the reference compound (≥0.700 compared with 0.081), which means the advantage of the wide therapeutic index of the new derivative. Additionally, our designed thiazolidinediones **12**, **16**, **17**, and **18** revealed better tolerability (−0.30 to 0.70) compared with 0.08 for the reference marketed anticancer agent. Finally, oral acute toxic doses of the new compounds (LD_{50}) are almost the same as that of the reference drug (~2.35 for our new thiazolidinediones compared with 2.40 of doxorubicin).

TABLE 2 ADMET profile of the four most active compounds and doxorubicin

Parameter	12	16	17	18	Doxorubicin
Molecular properties					
Molecular weight	564.019	526.401	540.428	598.464	543.525
LogP	5.444	5.9207	6.22912	6.0974	0.0013
Rotatable bonds	8	6	6	8	5
Acceptors	7	5	5	7	12
Donors	2	2	2	2	6
Surface area	232.707	214.640	221.005	243.010	222.081
Absorption					
Water solubility	−4.376	−3.489	−3.494	−3.607	**−2.915**
Caco-2 permeability	0.462	0.659	0.56	0.51	0.457
Intestinal abs. (human)	84.982	95.074	95.551	90.603	62.372
Skin permeability	−2.735	−2.735	−2.735	−2.735	−2.735
P-glycoprotein substrate	Yes	Yes	Yes	Yes	Yes
P-glycoprotein I inhibitor	Yes	Yes	Yes	Yes	No
P-glycoprotein II inhibitor	Yes	Yes	Yes	Yes	No
Distribution					
VDss (human)	0.051	0.09	0.124	0.174	1.647
Fraction unbound (human)	0.035	0.127	0.12	0.108	0.215
BBB permeability	−1.726	−1.503	−1.527	−1.911	−1.379
CNS permeability	−2.808	−1.725	−1.649	−2.637	−4.307
Metabolism					
CYP2D6 substrate	Yes	Yes	Yes	No	No
CYP3A4 substrate	Yes	Yes	Yes	Yes	No
CYP1A2 inhibitor	No	Yes	Yes	No	No
CYP2C19 inhibitor	Yes	Yes	Yes	Yes	No
CYP2C9 inhibitor	Yes	Yes	Yes	Yes	No
CYP2D6 inhibitor	No	No	No	No	No
CYP3A4 inhibitor	Yes	Yes	Yes	Yes	No
Excretion					
Total clearance	−0.530	−0.536	−0.592	−0.538	0.987
Renal OCT2 substrate	No	No	No	No	No
Toxicity					
AMES toxicity	No	No	No	No	No
Max. tolerated dose (human)	0.306	0.797	0.700	0.63	0.081
hERG I inhibitor	No	No	No	No	No
hERG II inhibitor	Yes	Yes	Yes	Yes	Yes
Oral rat acute toxicity (LD$_{50}$)	2.272	2.21	2.236	2.308	2.408
Oral rat chronic toxicity (LOAEL)	1.78	1.278	1.167	0.774	3.339
Hepatotoxicity	Yes	Yes	Yes	No	Yes
Skin sensitization	No	No	No	No	No
Tetrahymena pyriformis toxicity	0.292	0.319	0.322	0.298	0.285
Minnow toxicity	0.524	1.702	1.57	1.583	4.412

Abbreviation: ADMET, absorption, distribution, metabolism, excretion, and toxicity.

2.6 | Docking studies

In the present work, all modeling experiments were performed using Molsoft software. Each experiment used VEGFR-2 downloaded from the Brookhaven Protein Data Bank (PDB ID: 1YWN).[48]

The obtained results indicated that all studied ligands have similar position and orientation inside the recognized binding site of VEGFR-2, which reveals a large space bounded by a membrane-binding domain that serves as an entry channel for the substrate to the active site (Figure 6). In addition, the affinity of any small molecule can be considered as a unique tool in the field of drug design. There is a relationship between the affinity of organic molecules and free binding energy.[49–54] This relationship can contribute in the prediction and interpretation of the activity of the organic

compounds toward the specific target protein. The obtained results of the free energy of binding (ΔG) explained that most of these compounds had a good binding affinity toward the receptor and the computed values reflected the overall trend (Table 3).

The proposed binding mode of sorafenib revealed an affinity value of −95.66 kcal/mol and four H-bonds. The urea linker formed one H-bond with the key amino acid Glu883 (2.13 Å) through its NH group and one H-bond with Asp1044 (1.53 Å) through its carbonyl group. The *N*-methylpicolinamide moiety was stabilized by the formation of two H-bonds with Cys917, where the pyridine N atom formed one H-bond with the NH of Cys917 (2.46 Å) while its NH group formed one H-bond with the carbonyl of Cys917 (2.20 Å). The *N*-methylpicolinamide moiety occupied the hydrophobic groove formed by Leu1033, Gly920, Lys918, Cys917, Phe916, Glu915, Leu838, and Ala864. Moreover, the central phenyl ring occupied the hydrophobic pocket formed by Cys1043, Leu1033, Val914, Val897, and Lys866. Furthermore, the hydrophobic 3-trifluromethyl-4-chlorophenyl moiety attached to the urea linker occupied the hydrophobic pocket formed by Asp1044, Ile1042, His1024, Leu1017, Ile890, and Leu887 (Figure 7). The urea linker played an important role in the binding affinity toward the VEGFR-2 enzyme, where it was responsible for the higher binding affinity of sorafenib. These findings encourage us to use different linkers resembling urea of sorafenib, hoping to obtain potent VEGFR-2 inhibitors.

The proposed binding mode of compound **18** is virtually the same as that of sorafenib, which revealed an affinity value of −101.17 kcal/mol and six H-bonds. The carbonyl group of the acetamide linker formed one H-bond with Asp1044 (2.36 Å), while its NH group formed another H-bond with Glu883 (1.76 Å). The carbonyl group at position-2 of TZD formed one H-bond with Lys866 (2.71 Å). Moreover, the NH group of the carboxamide linker formed one H-bond with Asp1044 (2.61 Å). Furthermore, the carbonyl group of the distal ethyl ester moiety formed two H-bonds with Arg1025 (1.70 and 2.67 Å). The 2,4-dichlorophenyl moiety occupied the hydrophobic groove formed by

TABLE 3 The calculated ΔG (free energy of binding) and binding affinities for the ligands (ΔG in kcal/mol)

| Compound	ΔG (kcal/mol)	Compound	ΔG (kcal/mol)
7	−84.62	14	−92.92
8	−89.64	15	−96.25
9	−95.50	16	−96.37
10	−96.06	17	−98.76
11	−95.81	18	−101.17
12	−101.14	Sorafenib	−95.36
13	−86.54		

Leu1033, Gly920, Lys918, Cys917, Phe916, Glu915, Ala864, and Leu838. Moreover, the TZD moiety occupied the hydrophobic pocket formed by Cys1043, Leu1033, Val914, Val897, and Lys866. The hydrophobic phenyl tail occupied the hydrophobic pocket formed by Asp1044, Cys1043, Ile1042, Hie1024, Leu1017, Val897, Leu887, Lys866, and Glu883. Furthermore, the distal phenyl ring occupied the hydrophobic groove formed by Arg1025, Ile1023, Cys1022, Leu1017, Ile890, and Ile886. In contrast, the distal ethyl group of the ester moiety occupied the hydrophobic cleft formed by Cys1022, Lys1021, Arg1020, and Hie889 (Figure 8). These interactions of compound **18** may explain its highest anticancer activity.

As planned, the proposed binding mode of compound **12** is virtually the same as that of sorafenib, which revealed an affinity value of −101.14 kcal/mol and five H-bonds. The carbonyl group of the acetamide linker formed one H-bond with Asp1044 (2.42 Å) while its NH group formed another H-bond with Glu883 (1.74 Å). The carbonyl group at position-2 of TZD formed one H-bond with Lys866 (2.75 Å). Moreover, the NH group of the carboxamide linker formed one H-bond with Asp1044 (2.74 Å). Furthermore, the carbonyl group of the distal ethyl ester moiety formed one H-bond with Arg1025
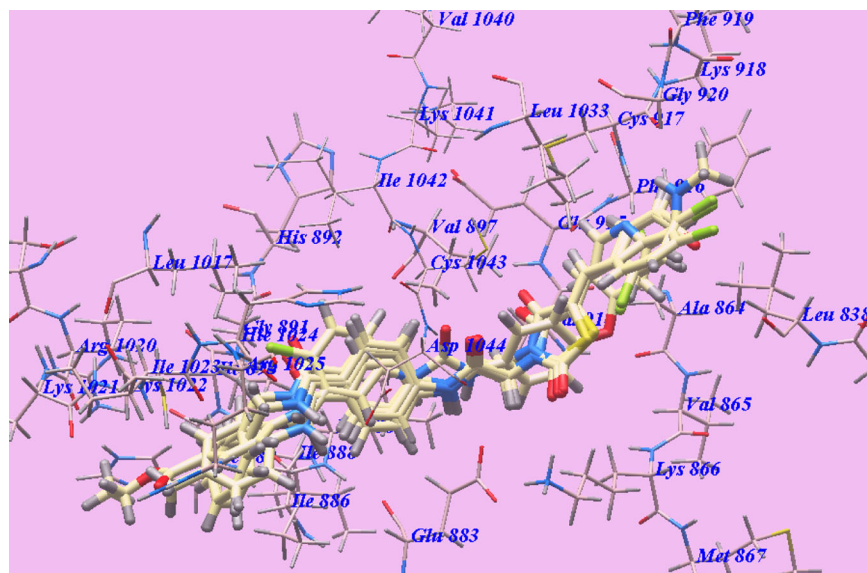
FIGURE 6 Superimposition of some docked compounds inside the binding pocket of 1YWN
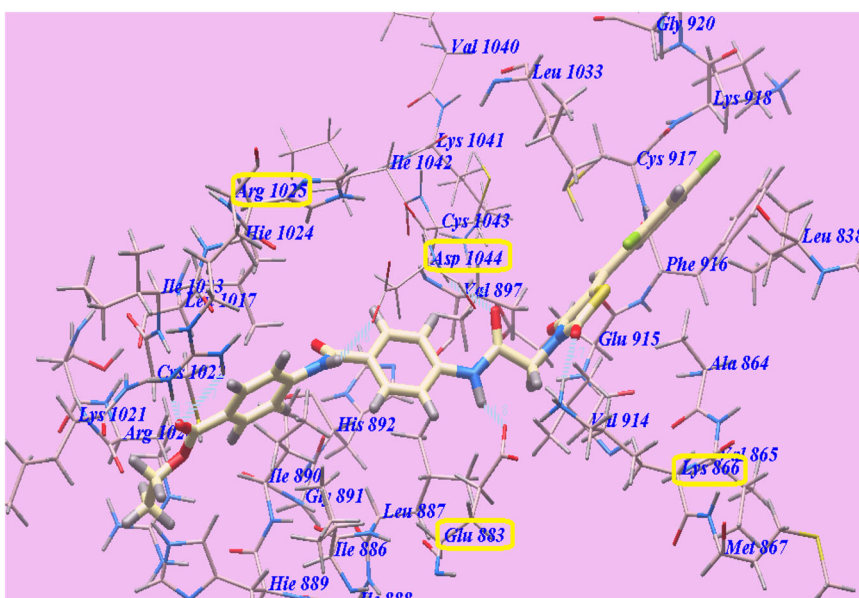
FIGURE 7 Predicted binding mode for sorafenib with 1WYN. H-bonded atoms are indicated by dotted lines
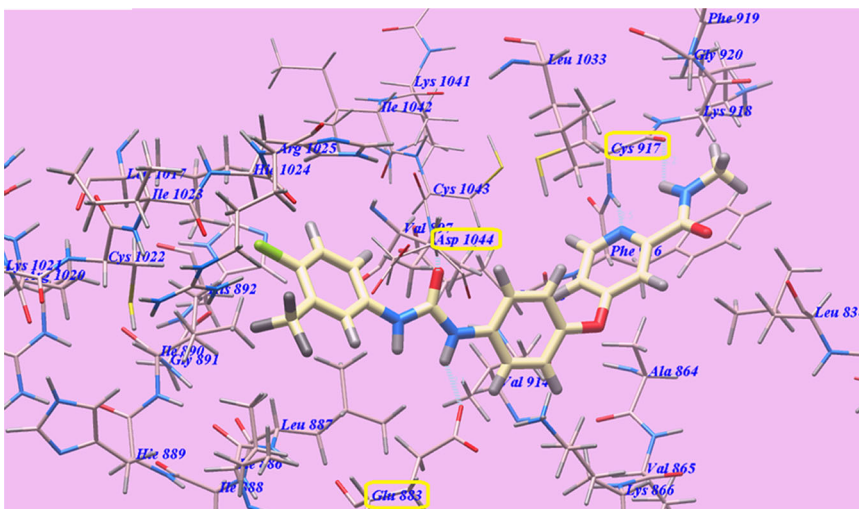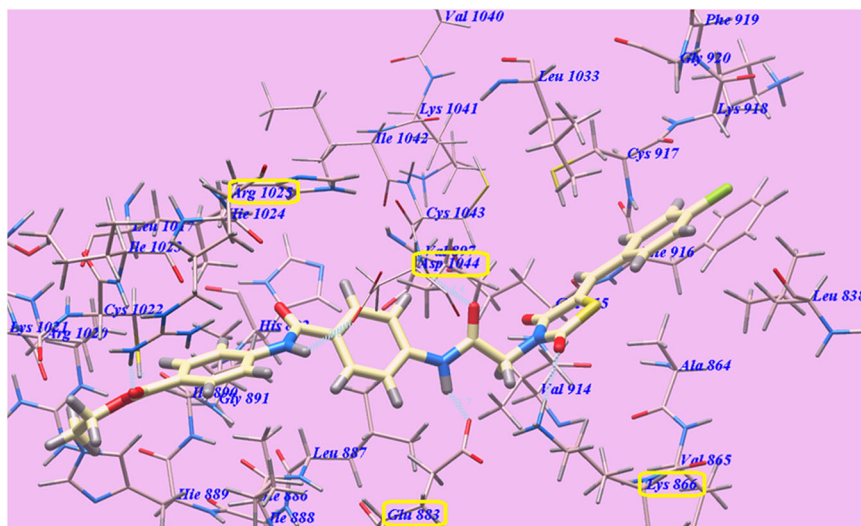

(1.92 Å). The 4-chlorophenyl moiety occupied the hydrophobic groove formed by Leu1033, Gly920, Lys918, Cys917, Phe916, Glu915, Ala864, and Leu838. Moreover, the TZD moiety occupied the hydrophobic pocket formed by Cys1043, Leu1033, Val914, Val897, and Lys866. The hydrophobic phenyl tail occupied the hydrophobic pocket formed by Asp1044, Cys1043, Ile1042, Hie1024, Leu1017, Val897, Leu887, Lys866, and Glu883. Furthermore, the distal phenyl ring occupied the hydrophobic groove formed by Arg1025, Ile1023, Cys1022, Leu1017, Ile890, and Ile886. In contrast, the distal ethyl group of the ester moiety occupied the hydrophobic cleft formed by Cys1022, Lys1021, Arg1020, and Hie889 (Figure 9). These interactions of compound **12** may explain its high anticancer activity.

The proposed binding mode of compound **17** is virtually the same as that of **18**, which revealed an affinity value of −98.76 kcal/mol and four H-bonds. The carbonyl group of the acetamide linker formed one H-bond with Asp1044 (2.15 Å), while its NH group formed another H-bond with Glu883 (1.88 Å). The carbonyl group at position-2 of TZD formed one H-bond with Lys866 (2.71 Å). Moreover, the NH group of the carboxamide linker formed one H-bond with Asp1044 (2.75 Å). The 2,4-dichlorophenyl moiety occupied the hydrophobic groove formed by Leu1033, Gly920, Lys918, Cys917, Phe916, Glu915, Ala864, and Leu838. Moreover, the TZD moiety occupied the hydrophobic pocket formed by Cys1043, Leu1033, Val914, Val897, and Lys866. The hydrophobic phenyl tail occupied the hydrophobic pocket formed by Asp1044, Cys1043, Ile1042, Hie1024, Leu1017, Val897, Leu887, Lys866, and Glu883. Furthermore, the distal methyl phenyl moiety occupied the hydrophobic groove formed by Arg1025, Ile1023, Cys1022, Leu1017, Ile890, and Ile886 (Figure 10). These interactions of compound **17** may explain its high anticancer activity.

FIGURE 8 Predicted binding mode for compound **18** with 1WYN
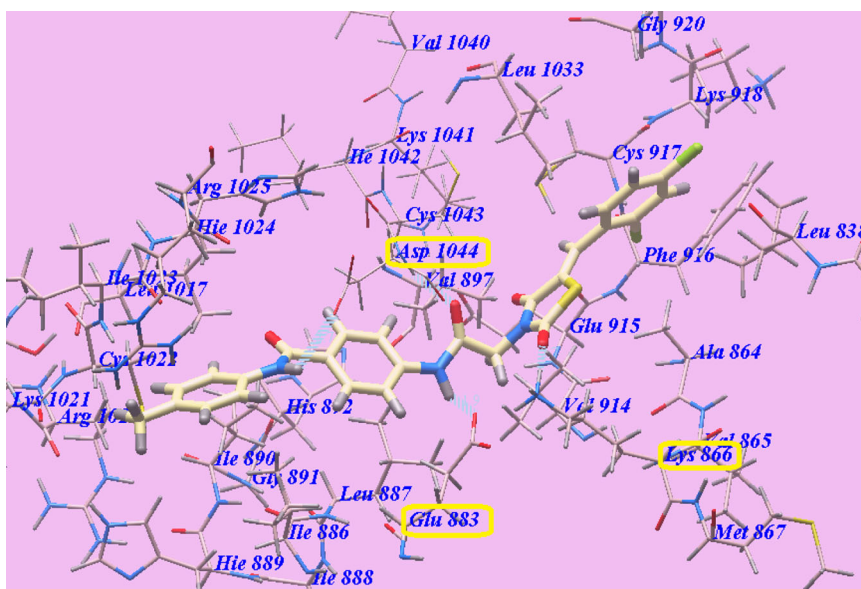
FIGURE 9 Predicted binding mode for compound **12** with 1WYN

The proposed binding mode of compound **16** is virtually the same as that of sorafenib and **18**, which revealed an affinity value of −96.37 kcal/mol and four H-bonds. The carbonyl group of the acetamide linker formed one H-bond with Asp1044 (2.22 Å), while its NH group formed another H-bond with Glu883 (1.95 Å). The carbonyl group at position-2 of TZD formed one H-bond with Lys866 (2.60 Å). Moreover, the NH group of the carboxamide linker formed one H-bond with Asp1044 (2.74 Å). The 2,4-dichlorophenyl moiety occupied the hydrophobic groove formed by Leu1033, Gly920, Lys918, Cys917, Phe916, Glu915, Ala864, and Leu838. Moreover, the TZD moiety occupied the hydrophobic pocket formed by Cys1043, Leu1033, Val914, Val897, and Lys866. The hydrophobic phenyl tail occupied the hydrophobic pocket formed by Asp1044, Cys1043, Ile1042, Hie1024, Leu1017, Val897, Leu887, Lys866, and Glu883. Furthermore, the distal benzyl moiety occupied the hydrophobic groove formed by Arg1025, Ile1023,

Cys1022, Leu1017, Ile890, and Ile886 (Figure 11). These interactions of compound **16** may explain its high anticancer activity.

From the obtained docking results (Table 1), we concluded that the acetamide linker occupied the same groove occupied by the urea linker of sorafenib and played the same role, which is essential for higher affinity toward VEGFR-2 enzyme. The lipophilicity of 2, 4-dichlorobenzylidene and 4-chlorobenzylidene moieties increased the hydrophobic interactions and consequently, affinities toward the VEGFR-2 enzyme. The TZD enables the new compounds to form new H-bond through its carbonyl group at position-2 with the essential amino acid Asp1044. Elongation of the structure played an important role in their VEGFR-2 inhibitory activities. The hydrophobic distal moiety and its linker which formed hydrogen bonding interactions with the amino acid Arg1025 and/or Arg1044, respectively also increased affinity toward VEGFR-2 enzyme.

FIGURE 10 Predicted binding mode for compound **17** with 1WYN

FIGURE 11 Predicted binding mode for compound **16** with 1WYN
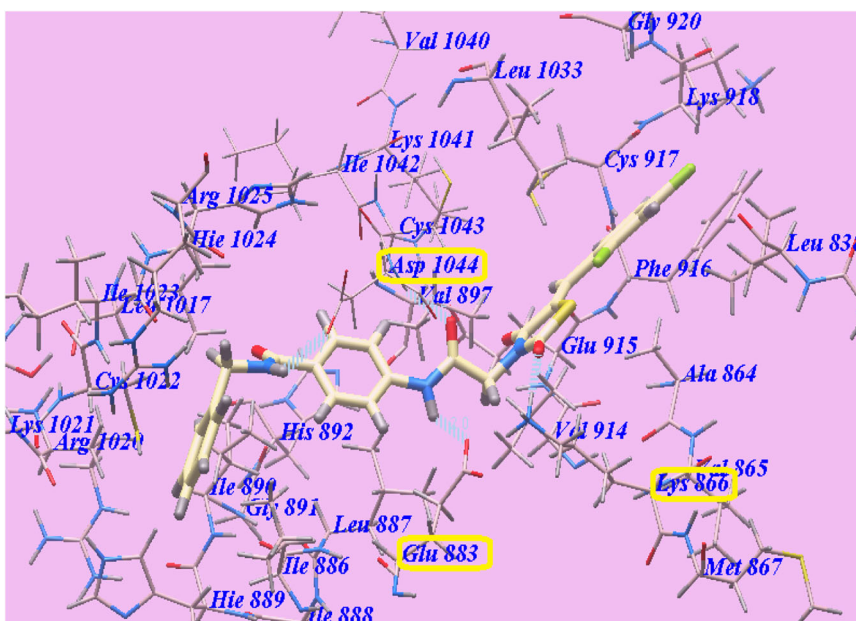
3 | CONCLUSION

Novel series of 5-([4-chloro/2,4-chloro]benzylidene)thiazolidine-2,4-dione derivatives **7**–**18** were designed, synthesized, and evaluated for their anticancer activity against three human tumor cell lines hepatocellular carcinoma (HepG2), colorectal carcinoma (HCT-116), and breast cancer (MCF-7) targeting VEGFR-2 enzyme. All the tested compounds showed variable anticancer activities. MCF-7 was the most sensitive cell line to the influence of the new derivatives. In particular, compounds **18**, **12**, **17**, and **16** were found to be the most potent derivatives over all the tested compounds against the HepG2, HCT116, and MCF-7 cancer cell lines with $IC_{50} = 9.16 \pm 0.9$, 8.98 ± 0.7, $5.49 \pm 0.5 \mu M$; 9.19 ± 0.5, 8.40 ± 0.7, $6.10 \pm 0.4 \mu M$; 10.78 ± 1.2, 8.87 ± 1.5, $7.08 \pm 1.6 \mu M$; and 10.87 ± 0.8, 9.05 ± 0.7, $7.32 \pm 0.4 \mu M$, respectively. Compounds **18** and **12** have nearly the same activities as sorafenib ($IC_{50} = 9.18 \pm 0.6$, 5.47 ± 0.3, and $7.26 \pm 0.3 \mu M$, respectively) against HepG2 cells, but slightly lower activity against HCT116 and slightly higher activity against MCF-7 cancer cell lines, respectively. Also, these compounds displayed lower activities than doxorubicin against HepG2 and HCT-116 cell lines but higher activity against MCF-7 cell line, respectively ($IC_{50} = 7.94 \pm 0.6$, 8.07 ± 0.8, and $6.75 \pm 0.4 \mu M$, respectively). However, compounds **17** and **16** exhibited lower activities than sorafenib, against HepG2 and HCT116, but nearly equipotent activity against MCF-7 cancer cell lines, respectively. Also, these compounds displayed lower activities than doxorubicin against the three cell lines. All the synthesized derivatives **7**–**18** were evaluated for their inhibitory activities against VEGFR-2. The tested compounds displayed high to medium inhibitory activity with IC_{50} values ranging from 0.17 ± 0.02 to $0.27 \pm 0.03 \mu M$. Among them, compounds **18**, **12**, **17**, and **16** potently inhibited VEGFR-2 at IC_{50} values of 0.17 ± 0.02, 0.17 ± 0.02, 0.18 ± 0.02, and $0.18 \pm 0.02 \mu M$, respectively, which are nearly more than the half of that of sorafenib IC_{50} value ($0.10 \pm 0.02 \mu M$). The molecular design was

performed to investigate the binding mode of the proposed compounds with the VEGFR-2 receptor. The data obtained from the docking studies were highly correlated with that obtained from the biological screening. The molecular design proved that the acetamide linker occupied the same groove occupied by the urea linker of sorafenib and played the same role, which is essential for a higher affinity toward VEGFR-2 enzyme. The lipophilicity of 2,4-dichlorobenzylidene and 4-chlorobenzylidene moieties increased the hydrophobic interactions and, consequently, affinities toward the VEGFR-2 enzyme. The TZD enables the new compounds to form new H-bond through its carbonyl group at position-2 with the essential amino acid Asp1044. Elongation of the structure played an important role in their VEGFR-2 inhibitory activities. The hydrophobic distal moiety and its linker, which formed hydrogen bonding interactions with the amino acid Arg1025 and/or Arg1044, respectively increased the affinity toward the VEGFR-2 enzyme. Furthermore, the ADMET profile was calculated for the four most active compounds in comparison with doxorubicin as a reference drug.

4 | EXPERIMENTAL

4.1 | Chemistry

4.1.1 | General

All melting points were carried out by open capillary method on a Gallenkamp Melting Point Apparatus at Faculty of Pharmacy, Al-Azhar University and were uncorrected. The infrared spectra were recorded on Pye Unicam SP1000 IR spectrophotometer at Microanalytical Unit, Faculty of Pharmacy, Cairo University using the potassium bromide disc technique. Proton magnetic resonance (^1H NMR) spectra were recorded on a Bruker 400 MHz NMR spectrophotometer at Microanalytical Unit,

Faculty of Pharmacy, Cairo University. ^{13}C NMR spectra were recorded on a Bruker 100 MHz NMR spectrophotometer at Microanalytical Unit, Faculty of Pharmacy, Cairo University. Tetramethylsilane was used as internal standard and chemical shifts were measured in δ scale (ppm). The mass spectra were carried out on Direct Probe Controller Inlet part to Single Quadrupole Mass Analyzer in Thermo Scientific GCMS Model ISQ LT using Thermo X-Calibur software at the Regional Center for Mycology and Biotechnology, Al-Azhar University. Elemental analyses (C, H, N) were performed on a CHN Analyzer at Regional Center for Mycology and Biotechnology, Al-Azhar University. All compounds were within ±0.4 of the theoretical values. The reactions were monitored by thin-layer chromatography (TLC) using TLC sheets precoated with UV fluorescent silica gel Merck 60 F254 plates and were visualized using a UV lamp and different solvents as mobile phases.

The original spectra of the investigated compounds are provided as Supporting Information. The InChI codes of the investigated compounds, together with some biological activity data, are also provided as Supporting Information.

TZD (**1**), 5-(2,4-dichlorobenzylidene)thiazolidine-2,4-dione, and 5-(4-chlorobenzylidene)-thiazolidine-2,4-dione (**2a,b**), the corresponding potassium salts (**3a,b**), 4-(2-chloroacetamido)-N-substitutedbenzamide derivative **6a–f** were obtained according to the reported procedures.[40,41,55–57]

4.1.2 | General method for the synthesis of 4-{2-[5-(4-chlorobenzylidene)-2,4-dioxothiazolidin-3-yl]-acetamido}-N-substitutedbenzamides 7–18

Equimolar quantities of the appropriate potassium salt **3a,b** (0.01 mol) and the appropriate 4-(2-chloroacetamido)-N-substitutedbenzamide derivative **6a–f** (0.01 mol) in dimethylformamide (DMF; 20 ml) were heated on the water bath for 5 hr. The reaction mixture was poured onto ice-water (200 ml) and stirred for 30 min. The obtained solid was filtered, washed with water, dried, and crystallized from ethanol to give the corresponding target compounds, **7–18**, respectively.

4-{2-[5-(4-Chlorobenzylidene)-2,4-dioxothiazolidin-3-yl]acetamido}-N-ethylbenzamide (7)

Yield, 85%; m.p. 242–244°C; IR$_{\nu max}$ (cm^{-1}): 3,240, 3,120 (2 NH), 3,012 (CH aromatic), 2,908 (CH aliphatic), 1,732, 1,685, 1,647 (4C=O); ^{1}H NMR (400 MHz, dimethyl sulfoxide [DMSO]-d_6): 1.11 (t, 3H, –NHCH$_2$CH$_3$), 3.27 (q, 2H, –NHCH$_2$CH$_3$), 4.56 (s, 2H, –NCH$_2$CO), 7.64 (d, 2H, Ar-H, H-3, H-5 of –C$_6$H$_4$Cl), 7.69–7.81 (m, 4H, Ar-H), 7.82 (d, 2H, Ar-H, H-3 and H-5 of –NHC$_6$H$_4$), 8.01 (s, 1H, C=CH-Ph), 8.36 (t, 1H, –NHCH$_2$CH$_3$, D$_2$O exchangeable), 10.63 (s, 1H, NH-benzamide, D$_2$O exchangeable); anal. calcd. for C$_{21}$H$_{18}$ClN$_3$O$_4$S (443.90): C, 56.82; H, 4.09; N, 9.47. Found: C, 56.71; H, 4.23; N, 9.68.

4-{2-[5-(4-Chlorobenzylidene)-2,4-dioxothiazolidin-3-yl]acetamido}-N-propylbenzamide (8)

Yield, 85%; m.p. 245–247°C; IR$_{\nu max}$ (cm^{-1}): 3,282, 3,194 (2 NH), 3,059 (CH aromatic), 2,870 (CH aliphatic), 1,747, 1,678, 1,631 (4C=O); ^{1}H NMR (400 MHz, DMSO-d_6): 0.85 (t, 3H, –NHCH$_2$CH$_2$CH$_3$), 1.46 (m, 2H, –NHCH$_2$CH$_2$CH$_3$), 3.17 (t, 2H, –CH$_2$CH$_2$CH$_3$), 4.56 (s, 2H, –NCH$_2$CO), 7.62 (m, 4H, Ar-H of –C$_6$H$_4$Cl), 7.69 (d, 2H, Ar-H H-2 and H-6 of –NHC$_6$H$_4$), 7.82 (d, 2H, Ar-H, H-3 and H-5 of –NHC$_6$H$_4$), 8.01 (s, 1H, C=CH-Ph), 8.36 (t, 1H, –NHCH$_2$CH$_2$CH$_3$, D$_2$O exchangeable), 10.63 (s, 1H, NH-benzamide, D$_2$O exchangeable); anal. calcd. for C$_{22}$H$_{20}$ClN$_3$O$_4$S (457.93): C, 57.70; H, 4.40; N, 9.18. Found: C, 58.02; H, 4.73; N, 9.45.

N-Butyl-4-{2-[5-(4-chlorobenzylidene)-2,4-dioxothiazolidin-3-yl]acetamido}benzamide (9)

Yield, 75%; m.p. 247–249°C; IR$_{\nu max}$ (cm^{-1}): 3,290, 3,120 (2 NH), 3,012 (CH aromatic), 2,908 (CH aliphatic), 1,743, 1,678, 1,635 (4C=O); ^{1}H NMR (400 MHz, DMSO-d_6): 0.92 (t, 3H, –CH$_2$CH$_2$CH$_2$CH$_3$), 1.28 (m, 2H, –CH$_2$CH$_2$CH$_2$CH$_3$), 1.46 (m, 2H, –CH$_2$CH$_2$CH$_2$CH$_3$), 3.23 (t, 2H, –CH$_2$CH$_2$CH$_2$CH$_3$), 4.55 (s, 2H, –NCH$_2$CO), 7.63 (m, 4H, Ar-H of –C$_6$H$_4$Cl), 7.69 (d, 2H, Ar-H, H-2 and H-6 of –NHC$_6$H$_4$), 7.81 (d, 2H, Ar-H, H-3 and H-5 of –NHC$_6$H$_4$), 8.01 (s, 1H, C=CH-Ph), 8.34 (s, 1H, –NHCH$_2$CH$_3$, D$_2$O exchangeable), 10.64 (s, 1H, NH-benzamide, D$_2$O exchangeable); anal. calcd. for C$_{23}$H$_{22}$ClN$_3$O$_4$S (471.96): C, 58.53; H, 4.70; N, 8.90. Found: C, 58.76; H, 4.89; N, 8.78.

N-Benzyl-4-{2-[5-(4-chlorobenzylidene)-2,4-dioxothiazolidin-3-yl]acetamido}benzamide (10)

Yield, 60%; m.p. 260–261°C; IR$_{\nu max}$ (cm^{-1}): 3,282, 3,190 (2 NH), 3,039 (CH aromatic), 2,920 (CH aliphatic), 1,747, 1,681, 1,647 (4C=O); ^{1}H NMR (400 MHz, DMSO-d_6): 4.46 (s, 2H, –CH$_2$Ph), 4.57 (s, 2H, –NCH$_2$CO), 7.23–7.36 (m, 5H, Ar-H, –C$_6$H$_5$), 7.55 (d, 2H, Ar-H, H-3 and H-5 of –C$_6$H$_4$Cl), 7.62 (d, 2H, Ar-H, H-2 and H-6 of –C$_6$H$_4$Cl), 7.69 (d, 2H, Ar-H, H-2 and H-6 of –C$_6$H$_4$), 7.88 (d, 2H, Ar-H, H-3 and H-5 of –C$_6$H$_4$), 8.02 (s, 1H, C=CH-Ph), 8.96 (s, 1H, –NHCH$_2$Ph, D$_2$O exchangeable), 10.65 (s, 1H, –NH-benzamide, D$_2$O exchangeable); anal. calcd. for C$_{26}$H$_{20}$ClN$_3$O$_4$S (505.97): C, 61.72; H, 3.98; N, 8.30. Found: C, 61.54; H, 4.07; N, 8.57.

4-{2-[5-(2,4-Chlorobenzylidene)-2,4-dioxothiazolidin-3-yl]acetamido}-N-(p-tolyl)benzamide (11)

Yield, 60%; m.p. 265–266°C; IR$_{\nu max}$ (cm^{-1}): 3,290, 3,190 (2 NH), 3,051 (CH aromatic), 2,935 (CH aliphatic), 1,743, 1,681, 1,635 (4C=O); ^{1}H NMR (400 MHz, DMSO-d_6): 2.28 (s, 3H, CH$_3$), 4.59 (s, 2H, –NCH$_2$CO), 7.14 (d, 2H, Ar-H, H-3 and H-5 of –C$_6$H$_4$CH$_3$), 7.61–7.71 (m, 8H, Ar-H), 7.95 (d, 2H, Ar-H, H-3 and H-5 of –C$_6$H$_4$CONH), 8.01 (s, 1H, C=CH-Ph), 10.08 (s, 1H, NH, –NHC$_6$H$_4$CH$_3$, D$_2$O exchangeable), 10.71 (s, 1H, NH, –NH-benzamide, D$_2$O exchangeable); anal. calcd. for C$_{26}$H$_{20}$ClN$_3$O$_4$S (505.97): C, 61.72; H, 3.98; N, 8.30. Found: C, 61.50; H, 4.16; N, 8.37.

Ethyl 4-(4-{2-[5-(4-chlorobenzylidene)-2,4-dioxothiazolidin-3-yl]acetamido}benzamido)benzoate (12)

Yield, 62%; m.p. 275–276°C; IR$_{\nu max}$ (cm^{-1}): 3,194, 3,109 (2 NH), 3,062 (CH aromatic), 2,939 (CH aliphatic), 1,739, 1,681, 1,631 (5C=O); ^{1}H NMR (400 MHz, DMSO-d_6): 1.30 (t, 3H, –COOCH$_2$CH$_3$), 4.27 (q, 2H, –COOCH$_2$CH$_3$), 4.59 (s, 2H, –NCH$_2$CO), 7.63 (d, 2H, Ar-H, H-3 and H-5 of –C$_6$H$_4$Cl), 7.69 (d, 2H, Ar-H, H-2 and H-6 of –C$_6$H$_4$Cl), 7.71 (d, 2H,

Ar-H, H-2 and H-6 of $-C_6H_4$), 7.95–8.00 (m, 6H, Ar-H), 8.02 (s, 1H, C=C**H**-Ph), 10.47 (s, 1H, N**H**, $-C_6H_4$CON**H**, D_2O exchangeable); ^{13}C NMR (100 MHz, DMSO-d_6): 14.69, 44.66, 60.92, 118.95, 119.99 (2), 122.16, 124.92, 129.46 (2), 129.78, 129.99 (2), 130.51 (3), 132.22 (2), 142.02, 132.33 (2), 132.89, 135.94, 144.16, 164.78, 165.65, 165.85, 167.61; anal. calcd. for $C_{28}H_{22}ClN_3O_6S$ (564.01): C, 59.63; H, 3.93; N, 7.45. Found: C, 59.89; H, 4.12; N, 7.53.

4-{2-[5-(2,4-Dichlorobenzylidene)-2,4-dioxothiazolidin-3-yl] acetamido}-N-ethylbenzamide (13)

Yield, 80%; m.p. 243–245°C; IR (KBr) νmax: 3,279, 3,066, 2,936, 1,751, 1,697 cm^{-1}; ^{1}H NMR (DMSO, 400 MHz): δ = 1.23 (t, 3H, $-CH_2CH_3$), 3.67 (q, 2H, $-CH_2CH_3$), 4.47 (s, 2H, $-NCH_2CO$), 7.24 (d, 1H, Ar-H, H-5 of $-C_6H_3$), 7.39–7.49 (m, 2H, Ar-H, H-2 and H-6 of $-C_6H_3$), 7.54–7.65 (m, 2H, Ar-H, H-2 and H-6 of $-C_6H_4$), 7.95–8.04 (m, 2H, Ar-H, H-3 and H-5 of $-C_6H_4$), 8.11 (s, 1H, C=C**H**-Ph), 9.01 (s, 1H, $-$N**H**CH_2CH_3, D_2O exchangeable), 10.68 (s, 1H, NH-C_6H_4, D_2O exchangeable); ^{13}C NMR (100 MHz, DMSO-d_6): 14.18, 44.89, 46.73, 111.51, 115.41, 118.29, 123.70, 126.93 (2), 127.81, 128.61, 129.19 (2), 132.97, 136.06, 136.58, 140.05, 142.96, 161.46, 166.55, 167.37; anal. calcd. for $C_{21}H_{17}Cl_2N_3O_4S$ (478.34): C, 52.73; H, 3.58; N, 8.78. Found: C, 52.59; H, 3.74; N, 9.07.

4-{2-[5-(2,4-Dichlorobenzylidene)-2,4-dioxothiazolidin-3-yl] acetamido}-N-propylbenzamide (14)

Yield, 80%; m.p. 246–248°C; IR (KBr) νmax 3,298, 3,059, 2,928, 1,740, 1,686, 1,670 cm^{-1}; ^{1}H NMR (DMSO, 400 MHz): δ = 0.89 (t, 3H, $-CH_2CH_2CH_3$), 1.50–1.56 (m, 2H, $-CH_2CH_2CH_3$), 3.22 (t, 2H, $-CH_2CH_2CH_3$), 4.56 (s, 2H, $-NCH_2CO$), 7.36 (d, 1H, Ar-H, H-5 of $-C_6H_3$), 7.44–7.51 (m, 2H, Ar-H, H-3 and H-6 of $-C_6H_3$), 7.53–7.59 (m, 2H, Ar-H, H-2 and H-6 of $-C_6H_4$), 7.63–7.66 (m, 2H, Ar-H, H-3 and H-5 of $-C_6H_4$), 7.82 (s, 1H, C=C**H**-Ph), 8.37 (s, 1H, $-$N**H**CH_2CH_2CH_3, D_2O exchangeable), 10.69 (s, 1H, NH-C_6H_4, D_2O exchangeable); anal. calcd. for $C_{22}H_{19}Cl_2N_3O_4S$ (492.37): C, 53.67; H, 3.89; N, 8.53. Found: C, 53.49; H, 4.12; N, 8.70.

N-Butyl-4-{2-[5-(2,4-dichlorobenzylidene)-2,4-dioxothiazolidin-3-yl] acetamido}benzamide (15)

Yield, 70%; m.p. 248–249°C; IR (KBr) νmax 3,267, 3,059, 2,932, 1,748, 1,693, 1,659 cm^{-1}; ^{1}H NMR (DMSO, 400 MHz): δ = 0.88 (t, 3H, $-CH_2CH_2CH_2CH_3$), 1.33 (m, 2H, $-CH_2CH_2CH_2CH_3$), 1.53 (m, 2H, $-CH_2CH_2CH_2CH_3$), 3.24 (t, 2H, $-CH_2CH_2CH_2CH_3$), 4.59 (s, 2H, $-NCH_2CO$), 7.53 (m, 3H, Ar-H, H-3, H-5 and H-6 of $-C_6H_3$), 7.67 (m, 2H, Ar-H, H-2 and H-6 of $-C_6H_4$), 7.85 (m, 2H, Ar-H, H-3 and H-5 of $-C_6H_4$), 7.97 (s, 1H, C=C**H**-Ph), 8.40 (s, 1H, $-$N**H**CH_2CH_2CH_3, D_2O exchangeable), 11.16 (s, 1H, NH-C_6H_4, D_2O exchangeable); anal. calcd. for $C_{23}H_{21}Cl_2N_3O_4S$ (506.40): C, 54.55; H, 4.18; N, 8.30. Found: C, 54.83; H, 4.29; N, 8.59.

N-Benzyl-4-{2-[5-(2,4-dichlorobenzylidene)-2,4-dioxothiazolidin-3-yl]acetamido}benzamide (16)

Yield, 65%; m.p. 262–264°C; IR (KBr) νmax 3,240, 3,055, 2,939, 1,739, 1,694 cm^{-1}; ^{13}C NMR (DMSO, 100 MHz): δ = 42.99, 44.83, 118.86, 127.12 (3), 127.72 (4), 128.68 (5), 129.03, 129.35, 129.67, 133.50, 133.61, 133.68, 140.35, 141.42, 163.92, 164.55, 166.12; anal. calcd. for $C_{26}H_{19}Cl_2N_3O_4S$ (540.42): C, 57.79; H, 3.54; N, 7.78. Found: C, 58.02; H, 3.71; N, 7.94.

4-{2-[5-(2,4-Dichlorobenzylidene)-2,4-dioxothiazolidin-3-yl] acetamido}-N-(p-tolyl)benzamide (17)

Yield, 65%; m.p. 270–272°C; IR (KBr) νmax 3,309, 3,152, 3,063, 2,928, 1,728, 1,687, 1,666 cm^{-1}; ^{1}H NMR (DMSO, 400 MHz): δ = 2.28 (s, 3H, CH_3), 4.58 (s, 2H, $-NCH_2CO$), 7.12–7.16 (m, 4H, Ar-H, $-C_6H_4CH_3$), 7.62–7.67 (m, 4H, Ar-H, $-C_6H_4$), 7.71 (m, 2H, Ar-H, H-5 of $-C_6H_3$ and C=C**H**-Ph), 7.95–7.99 (m, 2H, H-3 and H-6 of $-C_6H_3$), 10.08 (s, 1H, NH, $-$N**H**C_6H_4CH_3, D_2O exchangeable), 10.71 (s, 1H, NH, $-$N**H**C_6H_4CO, D_2O exchangeable); anal. calcd. for $C_{26}H_{19}Cl_2N_3O_4S$ (540.42): C, 57.79; H, 3.54; N, 7.78. Found: C, 57.96; H, 3.48; N, 8.12.

Ethyl 4-(4-{2-[5-(2,4-dichlorobenzylidene)-2,4-dioxothiazolidin-3-yl] acetamido}benzamido)benzoate (18)

Yield, 60%; m.p. 280–282°C; IR (KBr) νmax 3,233, 3,013, 2,939, 1,736, 1,686, 1,652 cm^{-1}; ^{13}C NMR (DMSO, 100 MHz): δ = 14.70, 44.63, 60.91, 118.94, 119.98 (2), 121.40, 124.91, 129.46 (2), 129.77, 129.92 (2), 130.51 (3), 130.70 (2), 131.33, 133.32, 134.20, 142.04, 144.18, 164.83, 165.65, 165.76, 165.84, 167.61; electron ionization mass spectroscopy (EIMS) m/z 602 [M$^+$+4] (0.88), 600 [M$^+$+2] (5.13), 598 [M$^+$] (7.38), 414 (28.29), 120 (100), 80 (10.49); anal. calcd. for $C_{28}H_{21}Cl_2N_3O_6S$ (598.45): C, 56.20; H, 3.54; N, 7.02. Found: C, 56.33; H, 3.70; N, 7.25.

4.2 | Biological assays

4.2.1 | In vitro cytotoxic activity

Cancer cells from different cancer cell lines, such as hepatocellular carcinoma (HepG2), breast cancer (MCF-7), and colorectal carcinoma (HCT-116), were purchased from American Type Cell Collection (ATCC, Manassas) and grown on the appropriate growth medium, Roswell Park Memorial Institute medium (RPMI 1640) supplemented with 100 mg/ml of streptomycin, 100 units/ml of penicillin, and 10% of heat-inactivated fetal bovine serum in a humidified, 5% (v/v) CO_2 atmosphere at 37°C cytotoxicity assay by MTT.

Exponentially growing cells from different cancer cell lines were trypsinized, counted, and seeded at the appropriate densities (2,000–1,000 cells/0.33-cm^2 well) into 96-well microtiter plates. Cells were then incubated in a humidified atmosphere at 37°C for 24 hr. Then, the cells were exposed to different concentrations of compounds (0.1, 10, 100, and 1,000 μM) for 72 hr. Then, the viability of treated cells was determined using MTT technique as follows. Cells were incubated with 200 μl of 5% MTT solution/well (Sigma-Aldrich, MO) and were allowed to metabolize the dye into colored insoluble formazan crystals for 2 hr. The remaining MTT solution was discarded from the wells and the formazan crystals were dissolved in 200 μl/well acidified isopropanol for 30 min, covered with aluminum foil and with continuous shaking using a MaxQ 2000 Plate Shaker (Thermo Fisher Scientific Inc., MI) at room temperature. Absorbance

was measured at 570 nm using a Stat FaxR 4200 Plate Reader (Awareness Technology Inc., FL). The cell viability was expressed as a percentage of control and the concentration that induces 50% of maximum inhibition of cell proliferation (IC_{50}) was determined using GraphPad Prism version 5 software (GraphPad Software Inc., CA).[42–44]

4.2.2 | In vitro VEGFR-2 kinase assay

The kinase activity of VEGFR-2 was measured using an antiphosphotyrosine antibody with the AlphaScreen system (PerkinElmer) according to the manufacturer's instructions.[58] Enzyme reactions were performed in 50 mM Tris–HCl pH 7.5, 5 mM $MnCl_2$, 5 mM $MgCl_2$, 0.01% Tween-20, and 2 mM dithiothreitol, containing 10 μM ATP, 0.1 μg/ml biotinylated poly-GluTyr (4:1), and 0.1 nM of VEGFR-2 (Millipore, UK). Before catalytic initiation with ATP, the tested compounds at final concentrations ranging from 0 to 300 μg/ml and enzyme were incubated for 5 min at room temperature. The reactions were quenched by the addition of 25 μl of 100 mM EDTA, 10 μg/ml AlphaScreen streptavidin donor beads and 10 μg/ml acceptor beads in 62.5 mM HEPES pH 7.4, 250 mM NaCl, and 0.1% bovine serum albumin. The plate was incubated in the dark overnight and then read by ELISA Reader (PerkinElmer). Wells containing the substrate and the enzyme without compounds were used as reaction control. Wells containing biotinylated poly-GluTyr (4:1) and enzyme without ATP were used as basal control. Percent inhibition was calculated by the comparison of compounds treated to control incubations. The concentration of the test compound causing 50% inhibition (IC_{50}) was calculated from the concentration–inhibition response curve (triplicate determinations) and the data were compared with sorafenib (Sigma-Aldrich) as standard VEGFR-2 inhibitor.

4.2.3 | Docking studies

In the present work, all the target compounds were subjected to a docking study to explore their binding mode toward the VEGFR-2 enzyme. All modeling experiments were performed using the Molsoft program, which provides a unique set of tools for the modeling of protein/ligand interactions. It predicts how small flexible molecules, such as substrates or drug candidates, bind to a protein of known 3D structure represented by grid interaction potentials (http://www.molsoft.com/icm_pro.html). Each experiment used the biological target VEGFR-2 downloaded from the Brookhaven Protein Data Bank (http://www.rcsb.org/pdb/explore/explore.do?structureId=1YWN). To qualify the docking results in terms of accuracy of the predicted binding conformations in comparison with the experimental procedure, the reported VEGFR-2 inhibitor drugs vatalanib and sorafenib were used as reference ligands.

CONFLICTS OF INTERESTS

The authors declare that there are no conflicts of interests.

ORCID

Khaled El-Adl http://orcid.org/0000-0002-8922-9770
Hamada S. Abulkhair http://orcid.org/0000-0001-6479-4573

REFERENCES

[1] G. Gasparini, R. Longo, M. Toi, N. Ferrara, *Nat. Clin. Pract. Oncol.* **2005**, *2*, 562.
[2] M. Potente, H. Gerhardt, P. Carmeliet, *Cell* **2011**, *146*, 873.
[3] L. Qin, J. L. Bromberg-White, C. N. Qian, *Adv. Cancer Res.* **2012**, *113*, 191.
[4] A. Bishayee, A. S. Darvesh, *Curr. Cancer Drug Targets* **2012**, *12*, 1095.
[5] H. Joshi, T. Pal, C. S. Ramaa, *Expert Opin. Investig. Drugs* **2014**, *23*, 501.
[6] U. Bhanushali, S. Rajendran, K. Sarma, P. Kulkarni, K. Chatti, S. Chatterjee, C. S. Ramaa, *Bioorg. Chem.* **2016**, *67*, 139.
[7] R. S. Kerbel, *N. Engl. J. Med.* **2008**, *358*, 2039.
[8] M. Shibuya, *Genes Cancer* **2011**, *2*, 1097.
[9] H. C. Spangenberg, R. Thimme, H. E. Blum, *Nat. Rev. Gastroenterol. Hepatol.* **2009**, *6*, 423.
[10] N. Ferrara, H. P. Gerber, J. LeCouter, *Nat. Med.* **2003**, *9*, 669.
[11] S. Koch, S. Tugues, X. Li, L. Gualandi, L. Claesson-Welsh, *Biochem. J.* **2011**, *437*, 169.
[12] D. K. Shah, K. M. Menon, L. M. Cabrera, A. Vahratian, S. K. Kavoussi, D. I. Lebovic, *Fertil. Steril.* **2010**, *93*, 2042. https://doi.org/10.1016/j.fertnstert.2009.02.059
[13] L. Nagarapu, B. Yadagiri, R. Bantu, C. G. Kumar, S. Pombala, J. Nanubolu, *Eur. J. Med. Chem.* **2014**, *71*, 91.
[14] Y. M. Ha, Y. J. Park, J. A. Kim, D. Park, J. Y. Park, H. J. Lee, J. Y. Lee, H. R. Moon, H. Y. Chung, *Eur. J. Med. Chem.* **2012**, *49*, 245.
[15] S. Faivre, C. Delbaldo, K. Vera, C. Robert, S. Lozahic, N. Lassau, C. Bello, S. Deprimo, N. Brega, G. Massimini, J. P. Armand, P. Scigalla, E. Raymond, *J. Clin. Oncol.* **2006**, *24*, 25.
[16] Q. Li, A. Al-Ayoubi, T. Guo, H. Zheng, A. Sarkar, T. Nguyen, S. T. Eblen, S. Grant, G. E. Kellogg, S. Zhang, *Bioorg. Med. Chem. Lett.* **2009**, *19*, 6042.
[17] R. Romagnoli, P. G. Baraldi, M. K. Salvador, M. E. Camacho, J. Balzarini, J. Bermejo, F. Estévez, *Eur. J. Med. Chem.* **2013**, *63*, 544. https://doi.org/10.1016/j.ejmech.2013.02.030
[18] C. Nastasă, R. Tamaian, O. Oniga, B. Tiperciuc, *Medicina* **2019**, *55*, 1.
[19] K. El-Adl, A.-G. A. El-Helby, H. Sakr, I. H. Eissa, S. S. A. El-Hddad, F. M. I. A. Shoman, *Bioorg. Chem.* **2020**, *102*, 104059. https://doi.org/10.1016/j.bioorg.2020.104059
[20] K. El-Adl, H. Sakr, M. Nasser, M. Alswah, F. M. A. Shoman, *Arch. Pharm.* **2020**, *353*, e2000079. https://doi.org/10.1002/ardp.202000079
[21] S. Takahashi, *Biol. Pharm. Bull.* **2011**, *34*, 1785.
[22] J. Kankanala, A. M. Latham, A. P. Johnson, S. Homer-Vanniasinkam, C. W. Fishwick, S. Ponnambalam, *Br. J. Pharmacol.* **2012**, *166*, 737.
[23] P. Wu, T. E. Nielsen, M. H. Clausen, *Trends Pharmacol. Sci.* **2015**, *36*, 422.
[24] S. Wilhelm, C. Carter, M. Lynch, T. Lowinger, J. Dumas, R. A. Smith, B. Schwartz, R. Simantov, S. Kelley, *Nat. Rev. Drug Discov.* **2006**, *5*, 835.
[25] A. Pircher, W. Hilbe, I. Heidegger, J. Drevs, A. Tichelli, M. Medinger, *Int. J. Mol. Sci.* **2011**, *12*, 7077. https://doi.org/10.3390/ijms12107077
[26] Q.-Q. Xie, H.-Z. Xie, J.-X. Ren, L.-L. Li, S.-Y. Yang, *J. Mol. Graphics Modell.* **2009**, *27*, 751.
[27] K. Lee, K.-W. Jeong, Y. Lee, J. Y. Song, M. S. Kim, G. S. Lee, Y. Kim, *Eur. J. Med. Chem.* **2010**, *45*, 542.
[28] R. N. Eskander, K. S. Tewari, *Gynecol. Oncol.* **2014**, *132*, 496.

[29] V. A. Machado, D. Peixoto, R. Costa, H. J. Froufe, R. C. Calhelha, R. M. Abreu, I. C. Ferreira, R. Soares, M.-J. R. Queiroz, *Bioorg. Med. Chem.* **2015**, *23*, 6497.

[30] J. Dietrich, C. Hulme, L. H. Hurley, *Bioorg. Med. Chem.* **2010**, *18*, 5738.

[31] A. Garofalo, L. Goossens, P. Six, A. Lemoine, S. Ravez, A. Farce, P. Depreux, *Bioorg. Med. Chem. Lett.* **2011**, *21*, 2106.

[32] M. A. Aziz, R. A. Serya, D. S. Lasheen, A. K. Abdel-Aziz, A. Esmat, A. M. Mansour, A. N. B. Singab, K. A. Abouzid, *Sci. Rep.* **2016**, *6*, 1. https://doi.org/10.1038/srep24460

[33] L. Zhang, Y. Shan, X. Ji, M. Zhu, C. Li, Y. Sun, R. Si, X. Pan, J. Wang, W. Ma, B. Dai, B. Wang, J. Zhang, *Oncotarget* **2017**, *8*, 104745. https://doi.org/10.18632/oncotarget.20065

[34] C. Viegas-Junior, A. Danuello, V. da Silva Bolzani, E. J. Barreiro, C. A. M. Fraga, *Curr. Med. Chem.* **2007**, *14*, 1829.

[35] A. A. El-Helby, R. R. A. Ayyad, H. Sakr, K. El-Adl, M. M. Ali, F. Khedr, *Arch. Pharm. Chem. Life Sci.* **2017**, *350*, e201700240. https://doi.org/10.1002/ardp.201700240

[36] A. A. El-Helby, H. Sakr, R. R. A. Ayyad, K. El-Adl, M. M. Ali, F. Khedr, *Anti-Cancer Agents Med. Chem.* **2018**, *18*, 1. https://doi.org/10.2174/1871520618666180412123833

[37] S. Rampogu, A. Baek, A. Zeb, K. W. Lee, *BMC Cancer* **2018**, *18*, 264. https://doi.org/10.1186/s12885-018-4050-1

[38] A. A. El-Helby, H. Sakr, I. H. Eissa, H. Abulkhair, A. A. Al-Karmalawy, K. El-Adl, *Arch. Pharm. Chem. Life Sci.* **2019**, *352*, e201900113. https://doi.org/10.1002/ardp.201900113

[39] A. A. El-Helby, H. Sakr, I. H. Eissa, A. A. Al-Karmalawy, K. El-Adl, *Arch. Pharm. Chem. Life Sci.* **2019**, *352*, e201900178. https://doi.org/10.1002/ardp.201900178

[40] S. Tahlan Sucheta, P. K. Verma, *Chem. Cent. J.* **2017**, *11*, 130.

[41] R. S. Bahare, S. Ganguly, K. Choowongkomon, S. Seetaha, *DARU J. Pharm. Sci.* **2015**, *23*, 1.

[42] T. Mosmann, *J. Immunol. Methods* **1983**, *65*, 55.

[43] D. A. Scudiero, R. H. Shoemaker, K. D. Paull, A. Monks, S. Tierney, T. H. Nofziger, M. J. Currens, D. Seniff, M. R. Boyd, *Cancer Res.* **1988**, *48*, 4827.

[44] F. M. Freimoser, C. A. Jakob, M. Aebi, U. Tuor, *Appl. Environ. Microbiol.* **1999**, *65*, 3727.

[45] C. A. Lipinski, F. Lombardo, B. W. Dominy, P. J. Feeney, *Adv. Drug Deliv. Rev.* **1997**, *23*, 3. https://doi.org/10.1016/S0169-409X(96)00423-1

[46] D. E. V. Pires, T. L. Blundell, D. B. Ascher, *pkCSM: J. Med. Chem.* **2015**, *58*, 4066. https://doi.org/10.1021/acs.jmedchem.5b00104

[47] A. Beig, R. Agbaria, A. Dahan, *PLOS One* **2013**, *8*, e68237. https://doi.org/10.1371/journal.pone.0068237

[48] S. A. H. El-Feky, H. A. Abd El-Fattah, N. A. Osman, M. Imran, M. N. Zedan, *J. Chem. Pharm. Res.* **2015**, *7*, 1154.

[49] B. Baum, M. Mohamed, M. Zayed, C. Gerlach, A. Heine, D. Hangauer, G. Klebe, *J. Mol. Biol.* **2009**, *390*, 56.

[50] L. Englert, A. Biela, M. Zayed, A. Heine, D. Hangauer, G. Klebe, *Biochim. Biophys. Acta* **2010**, *1800*, 1192.

[51] A. A. El-Helby, R. R. A. Ayyad, K. El-Adl, H. Sakr, A. A. Abd-Elrahman, I. H. Eissa, A. Elwan, *Med. Chem. Res.* **2016**, *25*, 3030.

[52] A. A. El-Helby, R. R. A. Ayyad, K. El-Adl, A. Elwan, *Med. Chem. Res.* **2017**, *26*, 2967.

[53] A. A. El-Helby, R. R. A. Ayyad, M. F. Zayed, H. S. Abulkhair, H. Elkady, K. El-Adl, *Arch. Pharm. Chem. Life Sci.* **2019**, *352*, e201800387. https://doi.org/10.1002/ardp.201800387

[54] A. A. El-Helby, R. R. A. Ayyad, H. Elkady, K. El-Adl, *Mol. Divers.* **2019**, *23*, 283. https://doi.org/10.1007/s11030-018-9871-y

[55] A. Mishra, G. V. Ghanshyam, B. Singh, J. Sweemit, S. Kumar, *Int. J. Pharm. Sci. Res.* **2010**, *1*, 41.

[56] A. A. El-Helby, R. R. Ayyad, H. M. Sakr, A. S. Abdelrahim, K. El-Adl, F. S. Sherbiny, I. H. Eissa, M. M. Khalifa, *J. Mol. Struct.* **2017**, *1130*, 333.

[57] S. A. Katke, S. V. Amrutkar, R. J. Bhor, M. V. Khairnar, *Int. J. Pharm. Sci. Res.* **2011**, *2*, 148.

[58] K. El-Adl, A.-G. A. El-Helby, H. Sakr, S. S. A. El-Hddad, *Arch. Pharm.* **2020**, *353*, e2000068. https://doi.org/10.1002/ardp.202000068

SUPPORTING INFORMATION

Additional supporting information may be found online in the Supporting Information section.